STABILITY AND CHAOS IN A LASER WITH AN INTRACAVITY SATURABLE ABSORBER

By:

Ing. Mario César Wilson Herrán

For the degree of

MASTER DEGREE IN SCIENCE (OPTICS)

Advisor

Dr. VICENTE ABOITES

León, Gto. México

August 2007

To my Family. . .

ACKNOWLEDGMENTS

At the end of any process, the possibility of pouring out the names of everything one is grateful to is an impossible task. Neither the time nor the will, would be enough to accomplish such a big undertaking, I should have to thank the time for rushing my steps, the sun for activating small melanin discharges in my skin, the moon for bringing back forgotten nostalgias, the sea for cutting up my existence each time a wave breaks somewhere in the world, my eyes for being an extension of sand, crystals and salt.

Best, mention the people and the crucial elements.

To my family for having blind faith in an idealistic fool.

To Linda for being the best that ever happen in my life.

To Doreen for her almost maternal patience.

To Dr. Vicente Aboites for supporting me with his knowledge and his wisdom.

To Dr. Alexander Kir'yanov, Dr. Victor Pinto, Dr. Alexander Pisarchik and Dr. Claudio Tebaldi for all the trouble they took so my thesis could come through.

To Dr. José Angel Canavati for all the teaching, I never would have found in a classroom.

To all the teachers that did their best not despair while sharing their knowledge with me.

To Laura for inciting me to do foolish things and to Guille for putting up with them.

To my classmates: Rigo, Sam, Dalia, Luis, Luis Adán, Ruth and Mario "el Tocayo", without them nothing would have been the same.

To Conacyt and CIO because their support made this dream possible.

To Poetry for being the balm for this obdurate romantic. To my pen for being my unconditional accomplice.

To everything that did anything so that this lost soul would take a step up in this infinite stairway that reaches nowhere.

Thanks to you all, sincerely.

Mario César

CONTENT

FIGURES LIST

CHAPTER 1 LASERS

CHAPTER 2 CHAOS

THESIS GENERAL OVERVIEW

This thesis presents a simulated study for a laser with an intracavity saturable absorber by the mean of the Statz-de Mars rate equations; this thesis is divided in two sections with four chapters.

Section one: Theoretical part

This part of the thesis gives the theoretical background of the realized work.

Chapter 1: Lasers

In this first chapter the lasers elemental concepts are boarded; e.g. optical gain, resonators, rate equations, lasing threshold.

Chapter 2: Chaos

This chapter undertakes the exposition of the basic chaos theory concepts that will be necessary for the realization and the results interpretation of this work are explained; e.g. critical points, dynamical systems, attractors.

Section two: Research part

In this part of the thesis the main problem is posed, boarded and solved

Chapter 3: Stability and chaos for the Statz-de Mars equations

This chapter begins with the theoretical bases of our problem, that is the Statz-de Mars equations and saturable filters; then the laser model is boarded, beginning with the statz-de Mars equations for a laser with an intracavity saturable absorber, finally, the equations system is solved in order to obtain the system's critical points and, the stable states of the system are plotted.

Chapter 4: Chaos results and conclusions

This final chapter presents the necessary conditions for the system to show chaotical behavior, in the same way, the final results and conclusions are discussed and future work is proposed.

CHAPTER 1

1.1 INTRODUCTION

A laser is a device that emits light through a specific mechanism for which the term laser is an acronym: light amplification by stimulated emission of radiation. This is a combined quantum-mechanical and thermodynamical process. As a light source, a laser can have various properties, depending on the purpose for which it is designed. A typical laser emits light in a highly directional and well-defined beam and with a specific wavelength (or color). This is in contrast to a light source such as the incandescent light bulb, which emits in almost all directions and over a wide wavelength spectrum. These properties are summarized in the term coherence.

1.2 INTERACTION RADIATION -MATTER

The Photons are individual units of energy. As a laser beam passes through an object, three possible fates await each photon:

1. It can penetrate and pass through the section of matter without interacting.
2. It can interact with matter and be completely absorbed as it gives away its energy.
3. It can interact and be scattered or deflected from its original direction and give away only part of its energy.

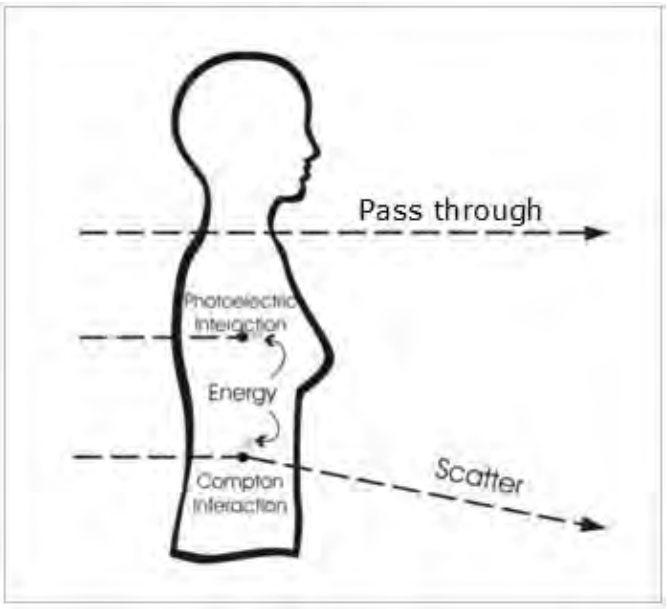

Figure 1.1 Photons entering an object, in this case a human body will either, pass through, be absorbed, or produce scattered radiation.

1.3 WHAT IS A LASER?

Broadly speaking, Lasers are devices that generate or amplify light, where “light” must be understood in the larger sense as any radiation ranging in wavelengths from the very long infrared region, merging with millimeter waves or even microwaves, up through the visible region and extending now to the vacuum ultraviolet and even X-ray regions. Lasers come in a great variety of forms, using many different kinds of pumping and excitation forms. The radiation beams emitted or amplified by a laser have remarkable properties of directionality, spectral purity, and intensity. These properties have already led to an enormous variety of applications, and others undoubtedly have yet to be discovered and developed.

A laser is composed of an active laser medium, or gain medium, and a resonant optical cavity. The gain medium transfers external energy into the laser beam. It is a material of controlled purity, size, concentration, and shape, which amplifies the beam by the quantum mechanical process of stimulated emission predicted by Albert Einstein. The gain medium is energized, or pumped, by an external energy source such as electricity and light; for example a flash lamp or another laser. The pumped energy is absorbed by the laser medium, placing some of its active centers into high-energy ("excited") quantum states. Active centers (which may be atoms, molecules, ions, etc.) can interact with light either by absorbing photons or by emitting photons. Emission can be spontaneous or stimulated. In the latter case, the photon is emitted in the same direction as the light that is passing by. When the number of active centers in one excited state exceeds the number of particles in some lower-energy state, population inversion is achieved and the amount of stimulated emission due to light that passes through is larger than the amount of absorption. Hence, the light is amplified.

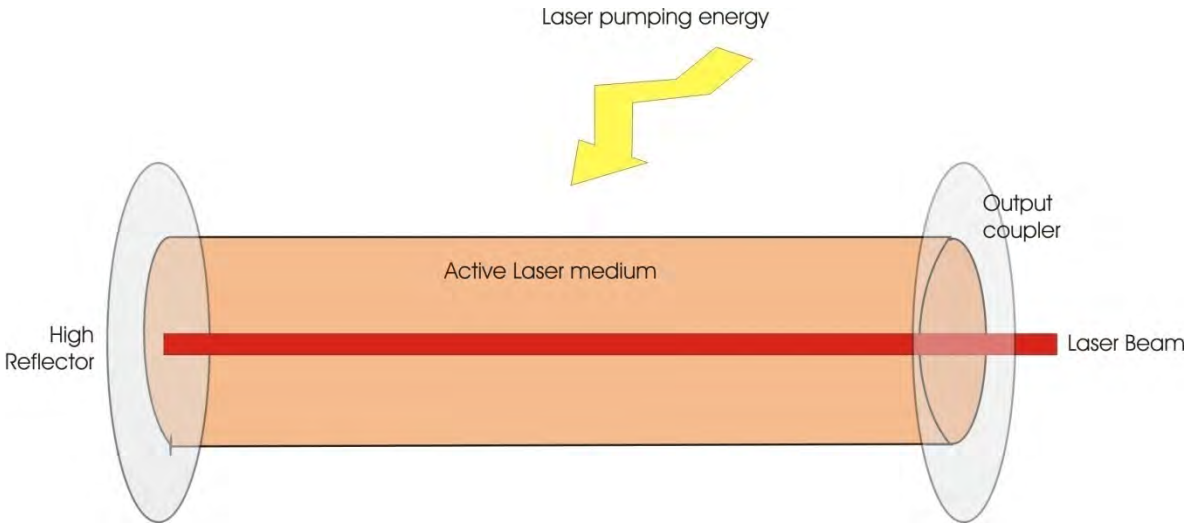

Figure 1.2 Principal elements of a Laser

The coherent light has to pass many times through the gain medium before it is emitted from the output aperture or lost to diffraction and absorption, so the light beam bounces on a set of mirrors that define the optical cavity as light circulates through the cavity, if the gain (amplification) in the medium is stronger than the resonator losses, its power can rise exponentially. The drawback is that each stimulated emission event returns an active center from its excited state to the ground state, reducing the capacity of the gain medium for further amplification. As this effect becomes stronger, the gain gets saturated. The balance between pump power, gain saturation and cavity losses produces an equilibrium value of the laser power inside the cavity; this equilibrium determines the operating point of the laser. If the chosen pump power is too small, the gain is not sufficient to overcome the resonator losses, and the laser will emit only spontaneous light. The minimum pump power needed to start a laser is called the lasing threshold. The gain medium will amplify any photons passing through it, regardless of direction; but only the photons aligned with the cavity will manage to pass more than once through the medium and so have significant amplification.

1.4 INDUCED AND SPONTANEOUS TRANSITIONS

Consider the interaction of an assembly of identical active centers with a radiator field whose energy density is distributed uniformly in frequency in the vicinity of the transition frequency. Let the energy density per unit frequency be ρ(ν) and take them as:

$$\left(W'_{21}\right)_i = B_{21}\rho(\nu)$$

$$\left(W'_{12}\right)_i = B_{12}\rho(\nu) \qquad (1.1)$$

where B_{21} and B_{12} are constants to be determinate. The total downward (2 →1) transition rate is the sum of the induced and spontaneous contributions

$$W'_{21} = B_{21}\cdot\rho(\nu) + A \qquad (1.2)$$

The total upward (1 → 2) transition rate is

$$W'_{12} = \left(W'_{12}\right)_i = B_{12}\rho(\nu) \qquad (1.3)$$

In this section we will find the expressions for B_{12} and B_{21}. Since the magnitude of the coefficients B_{21} and B_{12} depends on the atoms and not on the radiation field, must be considerate, the case where the atoms are in thermal equilibrium with a blackbody (thermal) radiation field at temperature T must be considered. In this case, the radiation density is given by as a Planck distribution

$$\rho(\nu) = \frac{8\cdot\pi\cdot n^3\cdot h\cdot\nu^3}{c^3}\left(\frac{1}{e^{\frac{h\cdot\nu}{K\cdot T}} - 1}\right) \tag{1.4}$$

Since at thermal equilibrium the average populations of level 2 and 1 are time constants, it follows that the number of 2→1 transitions in a given time interval is equal to the number of 1→2 transitions, that is,

$$N_2\cdot W'_{21} = N_1\cdot W'_{12} \tag{1.5}$$

where N_1 and N_2 are the population densities of level 1 and 2, respectively. Using (1.2) and (1.3) in (1.5), we obtain

$$N_2\cdot\left(B_{21}\cdot\rho(\nu) + A\right) = N_1\cdot B_{12}\cdot\rho(\nu)$$

substituting for ρ(ν) from (1.4),

$$N_2\cdot\left[B_{21}\cdot\frac{8\cdot\pi\cdot n^3\cdot h\cdot\nu^3}{c^3\left(e^{\frac{h\cdot\nu}{K\cdot T}} - 1\right)} + A\right] = N_1\left[B_{12}\cdot\frac{8\cdot\pi\cdot n^3\cdot h\cdot\nu^3}{c^3\left(e^{\frac{h\cdot\nu}{K\cdot T}} - 1\right)}\right] \tag{1.6}$$

Since the atoms are in thermal equilibrium, the ratio N_2/N_1 is given by the Boltzmann factor

$$\frac{N_2}{N_1} = \frac{g_2}{g_1}\cdot e^{-\frac{h\cdot\nu}{K\cdot T}} \tag{1.7}$$

Equating (N_2/N_1) as given by (1.6) and (1.7) gives

$$\frac{8n^3\cdot\pi\cdot h\cdot\nu^3}{c^3\left(e^{\frac{h\cdot\nu}{K\cdot T}} - 1\right)} = \frac{A\left(\frac{g_2}{g_1}\right)}{B_{12}\cdot\left(e^{\frac{h\cdot\nu}{K\cdot T}}\right) - B_{21}\left(\frac{g_2}{g_1}\right)} \tag{1.8}$$

The last equality can only be satisfied when

$$B_{12} = B_{21}\frac{g_2}{g_1} \tag{1.9}$$

and, simultaneously,

$$\frac{A}{B_{21}} = \frac{8\cdot\pi\cdot n^3\cdot h\cdot\nu^3}{c^3} \tag{1.10}$$

using (1.10), We can rewrite the induced transition rate (1.1) as

$$\left(W'_{21}\right)_i = \frac{A\cdot c^3}{8\pi\cdot n^3\cdot h\cdot\nu^3}\rho(\nu) = \frac{c^3}{8\pi\cdot n^3\cdot h\cdot\nu^3\cdot t_{spont}}\rho(\nu) \tag{1.11}$$

where $t_{spont} = 1/A$

Equation (1.11) gives the transition rate per atom due to a uniform (white) spectrum field with energy density per unit frequency ρ(ν). The main purpose of this section is the study of the transition rate $(W_{21})_i$ induced by a monochromatic field of frequency ν. The strength of interaction of a monochromatic field of frequency ν with an atomic transition is proportional to the lineshape function g(ν), so $(W'_{21})_i \alpha g(\nu)$. Furthermore, we would expect $(W_{21})_i$ to go over into $(W'_{21})_i$ as given by (1.11) if the spectral width of the radiation field is gradually increased from zero to a point at which it becomes large compared to the transition linewidth. The two requirements are satisfied if we take $(W_{21})_i$ to be

$$\left(W_{21}\right)_i = \frac{c^3\cdot\rho_\nu}{8\pi\cdot n^3\cdot h\cdot\nu^3\cdot t_{spont}}g(\nu) \tag{1.12}$$

where ρ_ν is the energy density of the electromagnetic field inducing the transitions. To show that $(W_{21})_i$ as given by (1.12) indeed goes over smoothly into (1.11) as the spectrum of the field broadens, we may consider the broad spectrum field is made up of a large number of closely spaced monochromatic components at ν_k with random phases and then adding the individual transition rates obtained from (1.12) obtaining

$$\left(W'_{21}\right)_i = \sum_{\nu_k}\left(W_{21}\right)_i(\nu_k) = \frac{c^3}{8\pi\cdot n^3\cdot h\cdot t_{spont}}\cdot\sum_k\frac{\rho_{\nu k}}{\left(\nu^3\right)_k}\cdot g(\nu_k) \tag{1.13}$$

where $\rho_{\nu k}$ is the energy density of the field component oscillating at ν_k. We can replace the summation of (1.13) by an integral if we replace $\rho_{\nu k}$ by ρ(ν) dν where ρ(ν) is the energy density per unit frequency; thus, (1.13) becomes

$$\left(W'_{21}\right)_i = \frac{c^3}{8\cdot\pi\cdot n^3\cdot h\cdot t_{spont}}\cdot\int_{-\infty}^{\infty}\frac{\rho(\nu)\,g(\nu)}{\nu^3}\,d\nu \tag{1.14}$$

In situations where ρ(ν) is sufficiently broad compared with g(ν), and thus the variation of ρ(ν)/ ν^3 over the region of interest can be neglected, we can pull ρ(ν)/ ν^3 outside the integral sign, obtaining

$$\left(W'_{21}\right)_i = \frac{c^3}{8\cdot\pi\cdot n^3\cdot h\cdot t_{spont}}\cdot\rho(\nu)$$

In agreement with (1.11), the normalization condition used was:

$$\int_{-\infty}^{\infty} g(\nu)\,d\nu = 1$$

Back to our main result, (1.12), we can rewrite it in terms of the optical wave intensity $I_\nu = c\rho_\nu/n$ (W/m^2) as

$$\left(W_{21}\right)_i = \frac{A\,c^2\cdot I_\nu}{8\cdot\pi\cdot n^2\cdot h\cdot\nu^3}\cdot g(\nu) = \frac{\lambda^2\cdot I_\nu}{8\pi n^2\cdot h\cdot\nu\cdot t_{spont}}\cdot g(\nu) \tag{1.15}$$

where c is the speed of light in the vacuum.

1.5 OPTICAL AMPLIFICATION

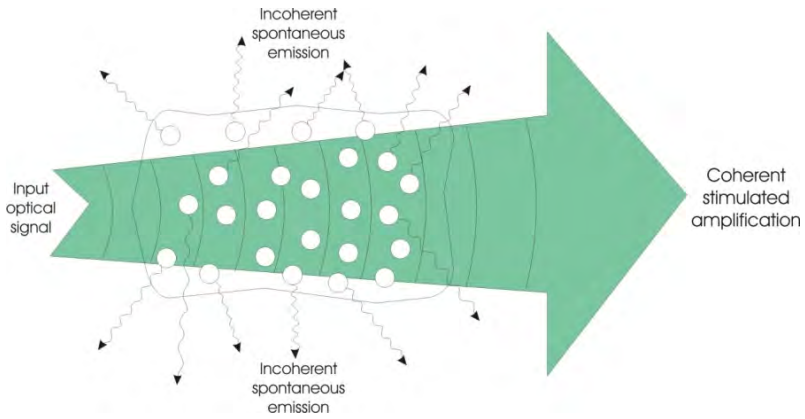

Figure 1.3 Optical amplification schemes

The energy of a bonded electron is proportional to its average distance to the atom's nucleus; however quantum mechanical effects force electrons to take on quantized positions in distinct orbitals. Thus, each electron is found in specific energy levels of an atom.

When electrons absorb energy either from light (photons) or from heat (phonons), they move farther away from the atomic nucleus but they are only allowed to absorb energy that will land them into specific energy levels. This leads to emission lines and absorption lines.

The Pauli Exclusion Principle forbids two electrons to have the same quantum numbers, making them fill up orbits further and further from the nucleus preventing them from all occupying the 1s orbital. When electrons absorb energy either from light (photons) or from heat (phonons), they move farther away from the atomic nucleus but they are only allowed to absorb energy that will land them into specific energy levels, which leads to emission and absorption lines.

When an electron is excited, it will not stay that way forever; there is an average lifetime for any particular energy level after which half of the electrons initially in that state will have decayed into a lower state. When such decay occurs, the energy difference between the level the electron was at and the new level must be released either as a photon or a phonon. When an electron decays due to "timeout" it is called "spontaneous emission." The phase associated with each emitted photon is random due to quantum mechanical properties of the atom's internal state. If a bunch of electrons were put into the same excited state somehow and then left to relax, the resulting radiation would be very spectrally limited to one wavelength but the individual photons would not be in phase with one another. This is also known as fluorescence.

In presence of other photons (i.e. of an external electromagnetic field) the atom's state will be affected. So that the quantum mechanical variables mentioned above do change. Specifically the atom will act like a small electric dipole which will oscillate with the external field. One of the consequences of this oscillation is that it encourages electrons to decay to the lower energy state. When this is done because of the interaction with other photons all the released photons are in phase and have the same direction. This is known as stimulated emission.

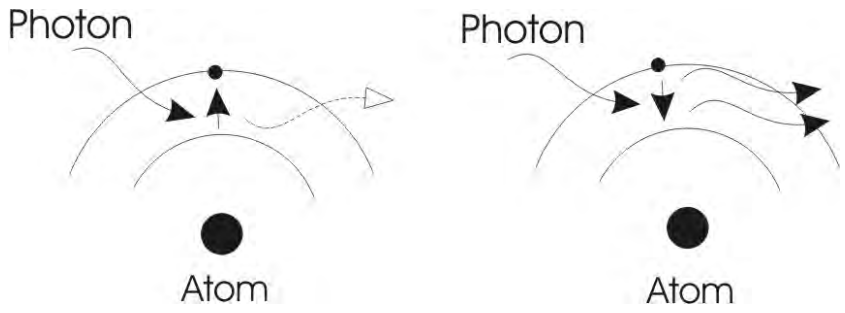

Figure 1.4 Photon descriptions of stimulated absorption and stimulated emission.

Stimulated emission can be modeled mathematically by considering an electron which may be in two electronic energy states, the ground state (1) and the excited state (2), with energies E_1 and E_2 respectively by the following equation:

$$E_2 - E_1 = h \cdot \nu_1 \tag{1.16}$$

where h is Planck's constant.

In a group of such atoms, if the number of atoms in the excited state is given by N, the rate at which stimulated emission occurs is given by:

$$\frac{\partial N}{\partial t} = -B_{21}\rho(\nu)N \tag{1.17}$$

where B_{21} is a proportionality constant (Einstein's coefficients) for this particular transition in this particular atom, and ρ(ν) is the radiation density of photons with ν frequency. The emission rate is thus proportional to the number of atoms in the excited state, N, and the density of the perturbing photons.

The two photons have the same polarization and, as a result, are totally coherent. It is this property that allows optical amplification to take place.

When an external source of energy stimulates atoms from the ground state into the excited state, it creates what is called a population inversion, so that when light of the appropriate frequency passes through the inverted medium, the photons stimulate the excited atoms to emit additional photons of the same frequency, phase, and direction, resulting in an amplification of the input intensity.

The population inversion, in units of atoms per cubic meter, is

$$\Delta N_{21} = \left(N_2 - \frac{g_2}{g_1} N_1 \right) \tag{1.18}$$

where g_1 and g_2 are the degeneracies of energy levels 1 and 2, respectively.

1.6 OPTICAL GAIN

The intensity (in watts per square meter) of the stimulated emission, if small enough not to have a significant effect on the magnitude of the population inversion, is governed by the following differential equation:

$$\frac{d}{dz}I = \sigma_{21}(\nu)\cdot\Delta N_{21}\cdot I(z) \tag{1.19}$$

Grouping the first two factors together, this equation simplifies as:

$$\frac{d}{dz}I = \gamma_0(\nu)\cdot I(z) \tag{1.20}$$

where $\gamma_0(\nu) = \sigma_{21}(\nu)\cdot\Delta N_{21}$ is the small-signal gain coefficient (in units of radians per meter). We can solve the differential equation using separation of variables:

$$\frac{dI}{I(z)} = \gamma_0(\nu)\cdot dz \tag{1.21}$$

Integrating, we find:

$$\ln\left(\frac{I(z)}{I_{in}}\right) = \gamma_0(\nu)\cdot z \tag{1.22a}$$

or

$$I(z) = I_{in}e^{\gamma_0(\nu)z} \tag{1.22b}$$

where $I_{in} = I(z = 0)$ is the optical intensity of the input signal (in watts per square meter).

Saturation Intensity

The saturation intensity I_s, defined as the input intensity at which the gain of the optical amplifier drops to exactly half of the small-signal gain can be computed it as:

$$I_s = \frac{h\nu}{\sigma(\nu)\cdot\tau_s} \tag{1.23}$$

where:

h is Planck's constant, and

τ_s is the saturation time constant, which depends on the spontaneous emission lifetimes of the various transitions between the energy levels related to the amplification.

General Gain Equation

The general form of the gain equation, which applies regardless of the input intensity, is derived from the general differential equation for the intensity I as a function of position z in the gain medium:

$$\frac{dI}{dz} = \frac{\gamma_0(\nu)}{1 + \bar{g}(\nu)\frac{I(z)}{I_S}} \cdot I(z) \tag{1.24}$$

where I_S stands for intensity. In order to solve the equation, we first rearrange it, separating the variables, intensity I and position z:

$$\frac{dI}{I(z)}\left[1 + \bar{g}(\nu)\frac{I(z)}{I_S}\right] = \gamma_0(\nu) \cdot dz \tag{1.25}$$

Integrating both sides, we obtain:

$$\ln\left(\frac{I(z)}{I_{in}}\right) + \bar{g}(\nu)\frac{I(z) - I_{in}}{I_S} = \gamma_0(\nu) \cdot z \tag{1.26a}$$

or

$$\ln\left(\frac{I(z)}{I_{in}}\right) + \bar{g}(\nu)\frac{I_{in}}{I_S}\left(\frac{I(z)}{I_{in}} - 1\right) = \gamma_0(\nu) \cdot z \tag{1.26b}$$

The gain G of the amplifier is defined as the optical intensity I at position z divided by the input intensity:

$$G = G(z) = \frac{I(z)}{I_{in}} \tag{1.27}$$

Substituting this definition into the prior equation (1.26b), we find the general gain equation:

$$\ln(G) + \bar{g}(\nu)\frac{I_{in}}{I_S}(G - 1) = \gamma_0(\nu) \cdot z \tag{1.28}$$

1.7 OPTICAL RESONATORS

Optical resonators are needed for two related main purposes: (1) to build up large field intensities at specific frequencies with moderate power inputs; (2) to act as spatial and frequency filters responding selectively to fields with prescribed spatial variation and frequency. The ability

of a resonator to perform these two tasks is measured by a universal figure of merit, the quality factor Q.

Light confined in a resonator will reflect multiple times from the mirrors, and due to the effects of interference, only certain patterns and frequencies of radiation will be sustained by the resonator, while the rest will be suppressed by destructive interference. Radiation patterns which are reproduced on every round-trip of the light through the resonator are the most stable, and are known as the resonator modes.

Resonator modes can be divided into two types: longitudinal modes, which differ in frequency from each other; and transverse modes, which may differ in both frequency and light intensity pattern. The fundamental transverse mode of a resonator is a Gaussian beam.

Generally optical cavities consist of two facing mirrors, either flat or spherical the simplest being the plane-parallel or Fabry-Perot cavity, consisting of two opposing flat mirrors. While simple, this arrangement is rarely used in large-scale lasers due the difficulty of alignment; the mirrors must be aligned parallel within a few seconds of arc, or "walk-off" of the intracavity beam will result in it spilling out of the sides of the cavity. However, this problem is much reduced for very short cavities with a small mirror separation distance ($L < 1$ cm).

For a resonator with two mirrors with radii of curvature R_1 and R_2, there are a number of common cavity configurations. If the two curvatures are equal to half the cavity length ($R_1 = R_2 = L / 2$), a concentric or spherical resonator results. This type of cavity produces a diffraction-limited beam waist in the centre of the cavity, with large beam diameters at the mirrors, filling the whole mirror aperture. Similar to this is the hemispherical cavity, with one plane mirror and one mirror of curvature equal to the cavity length.

A common and important design is the confocal resonator, with equal curvature mirrors equal to the cavity length ($R_1 = R_2 = L$). This design produces the smallest possible beam diameter at the cavity mirrors for a given cavity length, and is often used in lasers where the purity of the transverse mode pattern is important.

A concave-convex cavity has one convex mirror with a negative radius of curvature. This design produces no intracavity focus of the beam, and is thus useful in very high-power lasers where the intensity of the intracavity light might be damaging to the intracavity medium if brought to a focus.

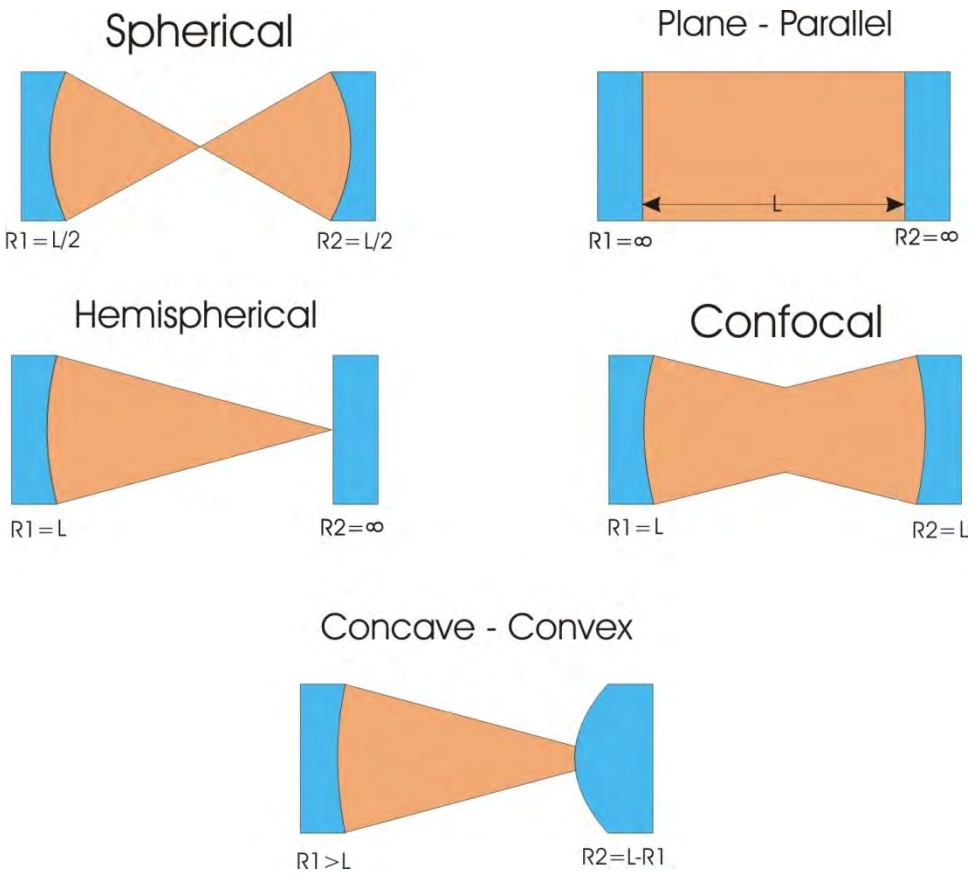

Figure 1.5 Types of two mirrors optical resonator

Stability in resonators

Only values for R_1, R_2, and L, in certain ranges allow periodic refocusing of the intracavity beam, producing stable resonators. If the cavity is unstable, the beam size will grow without limit, eventually growing larger than the size of the cavity mirrors and being lost. By using methods such as ray transfer matrix analysis, it is possible to calculate a stability criterion:

$$0 < \left(1 - \frac{L}{R_1}\right)\left(1 - \frac{L}{R_2}\right) < 1 \qquad (1.29)$$

Values which satisfy the inequality correspond to stable resonators.

If a stability parameter g is defined for each mirror, the stable regions can be shown graphically

$$g_1 = 1 - \frac{L}{R_1} \qquad g_2 = 1 - \frac{L}{R_2}$$

In the confocal cavity a ray, deviated from its original direction centered in the cavity, always returns to the center of the mirror. Preventing spontaneous emission from being amplified, this is important for a good beam quality and high power amplifiers. In wave optics this is expressed by the eigenvalue degeneration of the modes. On every turn to the left, the 0,0 mode and the 1,0 mode are 90° out of phase, but on the turn back, they are 180° out of phase. Interference of the modes then leads to a displacement.

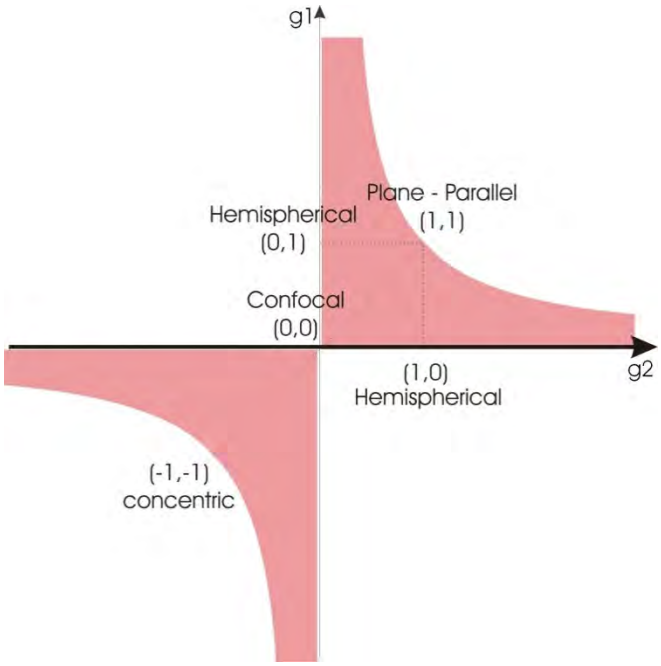

Figure 1.6 Stability Diagram for a two mirror resonator

1.8 LASER OSCILLATION CONDITION

We will “unleash” a Gaussian propagating beam mode inside an optical resonator made up of lenslike media and elements (including the gain medium), then trace its internal propagation using the ABCD law. The laser oscillation condition will emerge from the requirement that the beam reproduce itself in shape, amplitude, and phase, after each round trip.

We will use the Gaussian function:

$$q(z)\, e^{-i\theta(z)} \tag{1.30}$$

to characterize the beam at z. the parameter q(z) appearing in (1.30) is the complex beam radius defined as:

$$\frac{1}{q(z)} = \frac{1}{R(z)} - i\cdot\frac{\lambda}{\pi\cdot\omega^2(z)n} \tag{1.31}$$

and the factor $e^{-i\theta(z)}$ is the complex amplitude of the wave at z. θ is complex so that if we take $\theta = \theta_r + i\theta_i$, the beam power (at z relative to its value at z = 0 is given by $e^{2\theta_i(0)}$, and its phase at z by $-\theta_r(z)$.

The passage of a Gaussian beam through some lenslike element using the elements of a ray matrix, labeled by s, normally described as:

$$q_2 = \frac{A_s\cdot q_1 + B_s}{C_s q_1 + D_s} \tag{1.32}$$

is now modified to

$$q_2 e^{-i\theta_2} = \frac{A_s\cdot q_1 + B_s}{C_s q_1 + D_s} e^{-i(\theta_s+\theta_1)} \tag{1.33}$$

where $e^{-i\theta_s}$ is the complex amplitude transmission factor of the sth element. A lenslike element is now characterized by its A, B, C, D matrix as well as by its transmission factor $e^{-i\theta}$.

⊖ for a homogeneous medium extending between z_1 and z_2 is given by:

$$\theta_{hom} = k'(z_2 - z_1) - \left[(l + m + 1)\left(tan^{-1}\frac{z_2}{z_1} - tan^{-1}\frac{z_1}{z_0}\right)\right. \tag{1.34}$$

where k' is the complex propagation constant.

The ABCD matrix for a spherical mirror is:

$$\begin{pmatrix} 1 & 0 \\ \frac{-2}{R} & 1 \end{pmatrix}$$

And has a transmission factor $re^{-i\theta_m}$ where $(|r|)^2$ is the fraction of the incident power reflected by the mirror (reflectivity) and θ_m the phase shift upon reflection.

The propagation of a Gaussian beam through a sequence of N lenslike elements previously given by (1.32) can be described by:

$$q_{out} e^{-i\theta_{out}} = \frac{A \cdot q_{in} + B}{C \cdot q_{in} + D} e^{-i \cdot \theta_{in}} \cdot \prod_{s=1}^{N} e^{-i\theta_s} \tag{1.35}$$

where A, B, C, D are the elements of the product matrix obtained when multiplying the N individual matrices.

This formalism will be applied to derive the condition of laser oscillation. Consider the resonator shown in figure 1.7 that consists in two mirrors with (amplitude) reflectances $r_1 e^{-i \cdot \theta_{m1}}$ and $r_2 e^{-i \cdot \theta_{m2}}$, respectively. The resonator is filled with an amplifying medium whose complex propagation constant is k'.

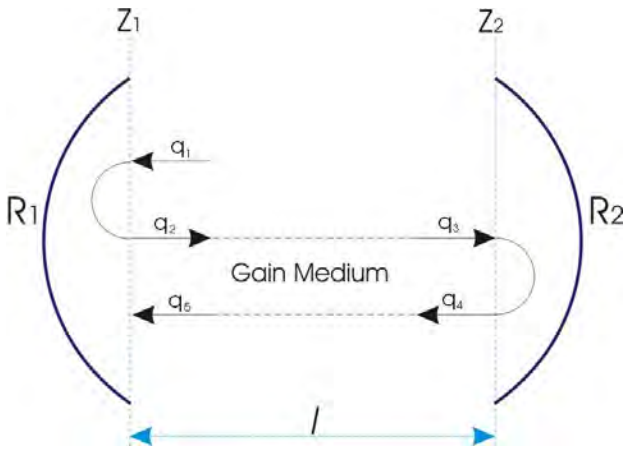

Figure 1.7 The propagation of a Gaussian beam inside an optical resonator

Following the evolution of the Gaussian laser beam through one round trip we obtain:

$$q_5 e^{-i \cdot \theta_5} = \frac{A \cdot q_1 + B}{C \cdot q_1 + D} \cdot e^{-i(\theta_1 + \theta)} \tag{1.36}$$

Using (1.34), (1.35) and taking l = m = 0, it yields

$$e^{-i \cdot \theta} = e^{-i \cdot 2\left[k' \cdot l - tan^{-1}\left(\frac{z_2}{z_0}\right) + tan^{-1}\left(\frac{z_1}{z_0}\right)\right]} r_1 \cdot r_2 e^{-i(\theta_{m1} + \theta_{m2})} \tag{1.37}$$

For self-reproducing oscillation, we require that the beam shape as well as its complex amplitude return to their original values after one round trip. This only happens when

$$q_5 = q_1 \tag{1.38a}$$

$$\theta_5 = \theta_1 + 2m\pi \tag{1.38b}$$

where m is an integer. The first condition (1.38a) is satisfied if:

$$q_1 = \frac{A \cdot q_1 + B}{C \cdot q_1 + D}$$

The second condition is satisfied when:

$$e^{-i \cdot \theta} = e^{-i \cdot 2 \cdot m \cdot \pi}$$

and using (1.37) it can be written as

$$e^{-i \cdot 2 \cdot m \pi} = e^{-i \cdot 2 \left[k' \cdot l - tan^{-1}\left(\frac{z_2}{z_0}\right) + tan^{-1}\left(\frac{z_1}{z_0}\right) \right]} r_1 r_2 e^{-i\left(\theta_{m1} + \theta_{m2}\right)} \tag{1.39}$$

known as the laser oscillation condition.

1.9 SATURATION

It has been established that the gain coefficient γ (ν) of a laser medium depends on the population difference ΔN; that ΔN depends on the transition rate W_i; and that W_i, in turn, depends on the radiation photon-flux density ϕ. It follows that the gain coefficient of a laser medium is dependent on the photon-flux density that is to be amplified. This is the origin of gain saturation.

We can part substituting the transition rate equation $W_i = \sigma(\nu)\phi$ on the steady-state population difference relation $N = \frac{N_0}{1+\tau_s W_i}$

$$N = \frac{N_0}{1 + \frac{\phi}{\phi_s(\nu)}} \tag{1.40}$$

where

$$\frac{1}{\phi_s(\nu)} = \tau_s \sigma(\nu) = \frac{\lambda^2}{8\pi} \frac{\tau_s}{t_{spon}} g(\nu) \tag{1.41}$$

This represents the dependence of the population difference ΔN on the photon-flux density ϕ. Now. Substituting (1.40) into the expression for the small-signal gain coefficient (1.20a) leads directly to the saturated gain coefficient for homogeneously broadened media:

$$\gamma(\nu) = \frac{\gamma_0(\nu)}{1 + \frac{\phi}{\phi_s(\nu)}} \tag{1.42}$$

The gain coefficient is a decreasing function of the photon-flux density ϕ, as illustrated in figure 1.8. The quantity $\phi_s(\nu) = 1/\tau_s\sigma(\nu)$ represents the photon-flux density at which the gain coefficient decreases to half its maximum value; it is therefore called the saturation photon-flux density. When $\tau_s \approx t_{spon}$ the interpretation of $\phi_s(\nu)$ is straightforward: roughly one photon can be emitted during each spontaneous emission time into each transition cross-sectional area [$\sigma(\nu)\phi_s(\nu)t_{spon} = 1$].

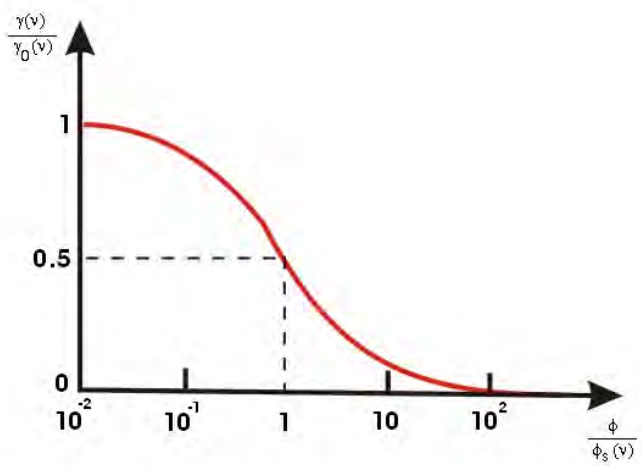

Figure 1.8 Saturation Gain Coefficient behaviors

1.10 RATE EQUATIONS

To make a laser work, an inverted population level must be achieved and maintained. For laser operation, excitation and decay rates of all of the different energy levels participating in the process must be balanced to maintain a steady-state inverted population for the radiative transition. The equations describing the change rates of the population densities N_1 and N_2 as a result of pumping, radiative, and non-radiative transitions are called the rate equations.

Consider the energy diagram of the figure 1.9. We focus on the levels 1 and 2, which have overall lifetimes τ_1 and τ_2, respectively, permitting transitions to lower levels. The lifetime of level 2 has two contributions: one associated with decay from 2 to 1 (τ_{21}), and the other (τ_{20}) associated with decay from 2 to all other lower levels. When several modes of decay are possible, the overall transition rate is a sum of the component transition rates. Since the rates are inversely proportional to the decay times, the reciprocals of the decay times must be added

$$\tau_2^{-1} = \tau_{21}^{-1} + \tau_{20}^{-1} \tag{1.43}$$

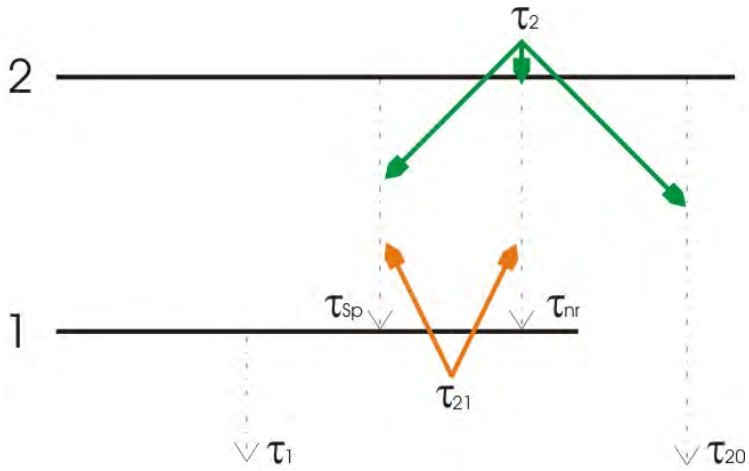

Figure 1.9 Energy levels 1 and 2 and their decay times

Multiple modes of decay therefore shorten the overall lifetime. Aside from the radiative spontaneous emission component (of time constant t_{sp}) in τ_{21}, a non-radiative contribution τ_{nr} may also be present (i.e. arising from a collision of the atom with the wall of the container thereby resulting in a depopulation), so that

$$\tau_{21}^{-1} = \tau_{sp}^{-1} + \tau_{nr}^{-1}$$

If a system like the illustrated in figure 1.9 is allowed to reach steady state, the population densities N_1 and N_2 will vanish by virtue of all the electrons ultimately decaying to lower levels.

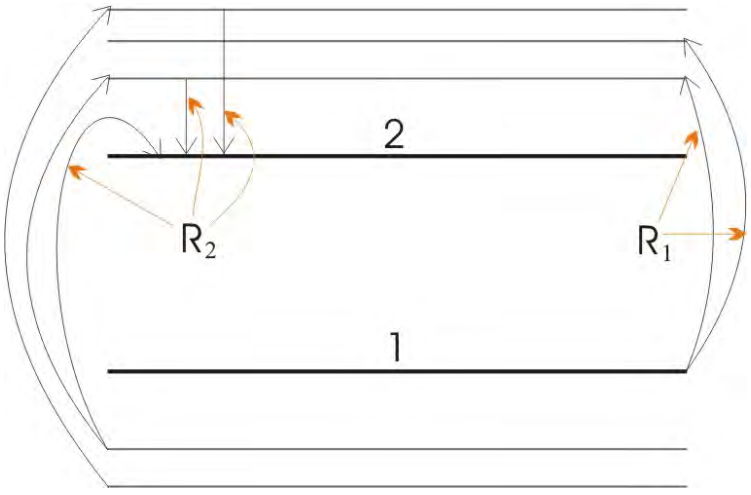

Figure 1.10 Energy levels 1 and 2 with surrounding higher and lower energy levels

Steady-state populations of levels 1 and 2 can be maintained, however, if energy levels above level 2 are continuously excited and leak downward into level 2, as shown in the more realistic energy level diagram of figure 1.10. Pumping can bring atoms from levels other than 1 and 2 out of level 1 and into level 2, at rates R_1 and R_2 (per unit volume per second), respectively, as shown in simplified form in figure 1.11. Consequently, levels 1 and 2 can achieve nonzero steady-state populations.

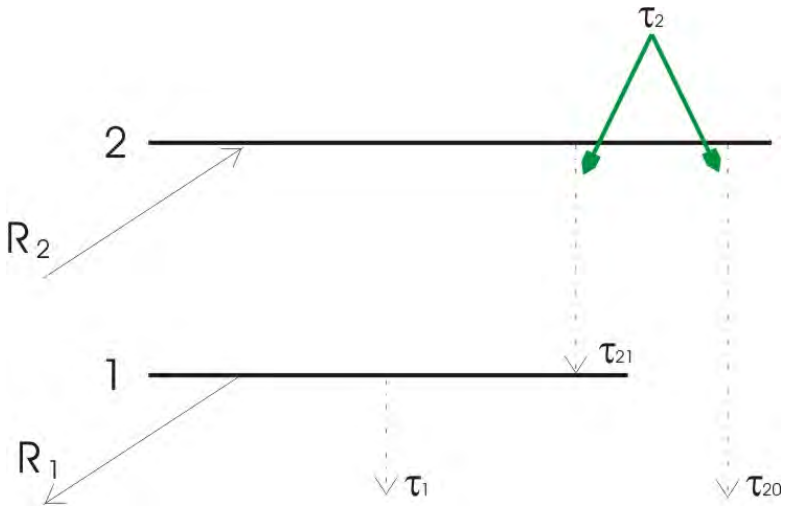

Figure 1.11 Energy levels 1 and 2 and their decay times. Level 1 increase by rate R_2 while level 1 decrease by rate R_1

Rate equations in the absence of amplifier radiation

The rates of increase of the population densities of levels 2 and 1 arising from pumping and decay are:

$$\frac{dN_2}{dt} = R_2 - \frac{N_2}{\tau_2} \tag{1.44}$$

$$\frac{dN_1}{dt} = -R_1 - \frac{N_1}{\tau_1} + \frac{N_2}{\tau_{21}} \tag{1.45}$$

Under steady state conditions $\left({}^{dN_1}/_{dt} = {}^{dN_2}/_{dt} = 0\right)$, (1.44) and (1.45) can be solved for N_1 and N_2, and the population difference $N = N_2 - N_1$ can be found. The result is

$$N_0 = R_2\tau_2\left(1 - \frac{\tau_1}{\tau_{21}}\right) + R_1\tau_1 \tag{1.46}$$

where the symbol N_0 represents the steady-state population difference N in the absence of amplified radiation.

A large gain coefficient clearly requires a large population difference (a large positive value of N_0). Equation (1.46) shows that this may be achieved by:

- Large R_1 and R_2
- Long τ_2 (but t_{sp}, which contributes to τ_2 through τ_{21}, must be sufficiently short so as to make the radiative transition rate large, as will be seen subsequently).
- Short τ_1 if $R_1 < (\tau_2/\tau_{21})R_2$.

The physical reasons underlying these conditions make good sense. The upper level should be pumped strongly and decay slowly so that it retains its population, while the lower level should dispose quickly of its population, that is depump strongly so that it quickly disposes of its population.

Rate equations in the presence of amplifier Radiation

The presence of radiation near the resonance frequency ν_0 enables transitions between levels 1 and 2 to take place by the processes of stimulated emission and absorption as well. These are characterized by the probability density $W_i = \phi\sigma(\nu)$, as shown in part 1.9 and illustrated in figure 1.12. The rate equations (1.44) and (1.45) must then be extended to include this source of population variation in each level:

$$\frac{dN_2}{dt} = R_2 - \frac{N_2}{\tau_2} - N_2 W_i + N_1 W_i \tag{1.47}$$

$$\frac{dN_1}{dt} = -R_1 - \frac{N_1}{\tau_1} + \frac{N_2}{\tau_{21}} + N_2 W_i - N_1 W_i \tag{1.48}$$

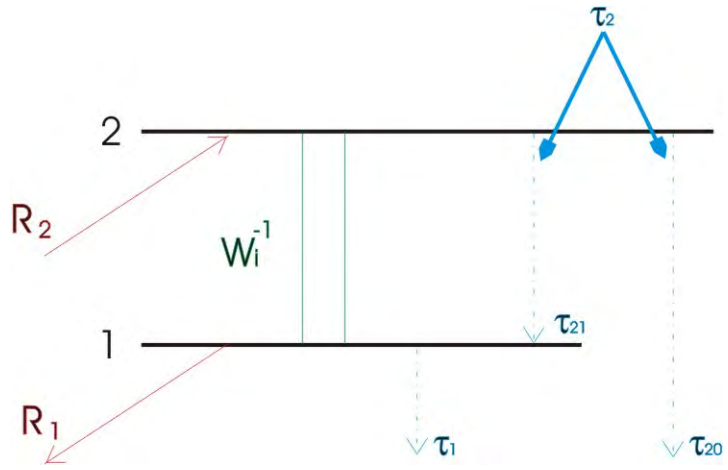

Figure 1.12 the population densities N_1 and N_2 ($cm^{-3}s^{-1}$) of atoms in energy levels 1 and 2 are determined by three processes: decay (b), pumping(r), and absorption and stimulated emission (g)

The population density of level 2 is decreased by stimulated emission from level 2 to level 1 and increased by absorption from level 1 to level 2. The spontaneous emission contribution is taken into account in τ_{21}.

Under steady state conditions $\left({}^{dN_1}/_{dt} = {}^{dN_2}/_{dt} = 0\right)$, (1.47) and (1.48) can be solved for N_1 and N_2, and the population difference $N = N_2 - N_1$ can be found. The result is

$$N = \frac{N_0}{1+\tau_s W_i} \tag{1.49}$$

$$\tau_s = \tau_2 + \tau_1\left(1 - \frac{\tau_2}{\tau_{21}}\right) \tag{1.50}$$

where N_0 is the steady-state population difference in the absence of amplified radiation, given by (1.46). The characteristic time τ_s is always positive since $\tau_2 \leq \tau_{21}$.

In the absence of amplified radiation, $W_i = 0$ so that (1.49) provides $N = N_0$, as expected. Because τ_s is positive, the steady-state population difference in the presence of radiation has always a smaller absolute value than in the absence of radiation, i.e. $|N| \leq |N_0|$. If the radiation is sufficiently weak so that $\tau_s W_i \ll 1$ (the small signal approximation), we may take $N \approx N_0$. As the radiation becomes stronger, W_i increases and N approaches zero regardless of the initial sign of N_0, as shown in figure 1.13. This arises because stimulated emission and absorption dominate the interaction when W_i is very large and they have equal probability densities. It is apparent that even very strong radiation cannot convert a negative population difference into a positive population difference, nor vice versa. That quantity τ_s plays the role of a saturation time constant, is evident from figure 1.13.

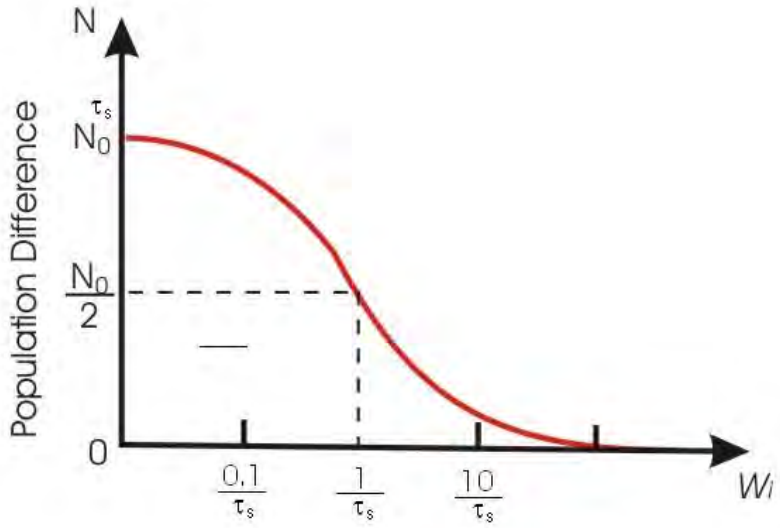

Figure 1.13 Depletion of the steady-state population difference $N = N_2 - N_1$ as the rate of absorption and stimulated emission W_i increases.

1.12 FIRST CHAPTER REFERENCES

- A.E. SIEGMAN, **LASERS**, University Science Books, 1986
- O. SVELTO, **PRINCIPLES OF LASERS**, Fourth edition, Springer, 1989
- BAHAA E. A. SALEH, **FUNDAMENTALS OF PHOTONICS**, John Wiley & sons, 1991
- A. YARIV, **QUANTUM ELECTRONICS**, third edition, John Wiley & sons, 1989
- V. ABOITES, **LÁSERES**, CIO, 1991
- L. TARASSOV, **PHYSIQUE DES PROCESSUS DANS LES GÉNÉRATEURS DE RAYONNEMENT OPTIQUE COHÉRENT**, Éditions MIR, 1981
- H.HAKEN, **LASER LIGHT DYNAMICS**, North Holland Physics Publishing, 1985
- J. VERDEYEN, **LASER ELECTRONICS**, Third edition, Prentice Hall, 1995

CHAPTER 2

2.1 INTRODUCTION

Upon hearing the word chaos, one's mind usually conjectures a place of total disorder and confusion. This is the usual meaning of the word in normal usage. However, there has been a literal explosion of scientific interest in chaos and how to control it or at least understand it. If the term chaos really implied total disorder or randomness, there would probably be no point in studying the phenomenon. However, in technical literature, the term chaos means something that appears to be random and disordered but is actually deterministic in nature, meaning that it is precisely controlled by natural laws. The apparent disorder arises from an extreme sensitivity to initial conditions, much like the path of the ball in a pinball machine seeming to defy human control. This chapter discusses the principal concepts and meanings involved in the Chaos science.

2.2 WHAT IS CHAOS?

Many people believe that twentieth century science will be remembered for three main theories: quantum mechanics, relativity, and chaos. Chaos theory is a blanketing theory that covers all aspects of science, hence, it shows up everywhere in the world today: mathematics, physics, biology, finance, and even music. Where classical sciences end, chaos is only beginning.

The term chaos theory is used widely to describe an emerging scientific discipline whose boundaries are not clearly defined. The terms complexity theory and complex systems theory provide a better description of the subject matter, but the term chaos theory will be used throughout this work as it is more widely accepted.

Chaos theory is a developing scientific discipline which is mainly focused on the study of nonlinear systems. To understand chaos theory, we must first have a grasp upon its roots: systems and the term nonlinear.

The first term, system, can be defined as the understanding of the relationship between things which interact. To better understand this idea, we will examine the example of a pile of stones. The pile is a system which interacts based upon how they were piled. If their initial piling is not in balance, the interaction results in their movement until they find a condition under which they are in balance. A group of stones which do not touch each other, however, are not a system because the interaction between is so minute, it can be considered non-existent.

Another important aspect (in dealing with systems) is that systems can be modeled. In other words, systems can be created to (which will) theoretically replicate the original system's behavior. Following the pile of stones example, one could take a second group of stones which are identical to the first group, pile them in exactly the same way as the first group, and predict that they will fall down into the exact same configuration as the first group. Similarly, a mathematical model, based upon Newton's law of gravity, could be used to predict how piles of same and different types will interact. Generally speaking, mathematical modeling is the key to modeling systems, although it is not the only way.

The second term, nonlinear, has to do with the type of mathematical model used to describe a system. Until the recent growth of interest in chaos theory, hence nonlinear systems, most models were analyzed as though they were linear systems. In other words, when the mathematical models were drawing in a graph format, the results appeared as a straight line. Calculus was Newton's mathematical method for showing change in systems within the context of a straight line and statistics, regression analysis in particular, is a process of converting nonlinear data into a linear format for further analysis and prediction.

Linear systems are easy to generate and simple to work with because they are very predictable. If for example, you think of a factory as a linear system, you could predict that by adding a certain number of people, or a certain amount of inventory to the factory, the number of pieces produced by the factory would be increased by a comparable amount. However, as most managers know, factories don't operate this way, changing the number of people, inventory, or any other variable in the factory would produce widely differing results on a day to day basis from a linear model prediction. This happens because, actually, factories are nonlinear systems, as are most systems (found in life). When dealing with real systems and try to make a mathematical model, their graphical representations usually are not straight lines and the system's behavior is not so easy to predict.

Prior to the development of chaos theory, most scientific studies attempted to understand the world using linear models. Beginning with the work of Sir Isaac Newton, physics has been provided the processes for modeling nature, and the mathematics associated with them have been linear in nature. Afterwards, when a prediction usually held, but in a particular study, the results seemed strange and did not match, the failure was blamed on experimental error, otherwise known as noise

Since research into complex systems is being done, we now know that noise holds actually important information about the experiment. When noise is taken into account in the graph results, the graph no longer appears as a straight line, nor are its points as predictable. At one time, this noise was referred to as the chaos in the experiment. The process of studying the noise in an experiment is one of the major aims of chaos theory

Another important word which has been used repeatedly is complex. What is the determining factor making one system more complex than another? The complexity of a system is

defined by the complexity of the model necessary to effectively predict the behavior of the system. The more alike the model and the actual system are, the more complex the system is considered to be. Weather is the most complex system example there is, since it can only be modeled with an exact duplicate of itself. On the other hand, a simple system to model is to predict the amount of time it takes for a train to travel from point A to point B, assuming a constant velocity and no stops in between. To predict the time we need only know the speed of the train and the distance between the two points. The formula is simple: d/v. Our old example of the pile of stones, which at first glance may look like a simple system, is actually very complex. If your goal was to predict the eventual location of each individual stone, then you will have to have very detailed information about each stone: their shape, weight, and the exact starting location. Any little difference between the shape of one stone in the model and the actual stone, will likely produce very different results making predictability very difficult thus making the system highly complex.

Sensitive Dependence on Initial Conditions

An essential element of a complex system is unpredictability. This unpredictability is generated by what Lorenz called sensitivity to initial conditions. This concept implies that when dealing with a complex, nonlinear system, a very small change in the starting conditions will result in dramatically different outputs.

This phenomenon is commonly known as the butterfly effect. As mentioned above, to accurately predict the weather, an exact replica of the earth would needed, so that failing to take into account a butterfly flapping its wings in a distant country could cause the model to fail to predict a thunderstorm over our home town in several weeks.

Because of extreme dependence on initial conditions, the general rule for complex systems is that one cannot create a model that will accurately predict outcomes. However, one can create models which simulate the processes that the system will go through to create the models. This realization is impacting many activities in business, as it raises considerable questions about the value of creating organizational visions and mission statements as current practice asks for.

The concept of sensitive dependence on initial conditions has strong mathematical roots. Suppose we have to points X_0 and X_1, on a circle, representing the correct starting value and are very close to being correct value for a variable in the model of a system T. We assume that the difference between the two numbers is represented by the distance d between the points on the circle, in order to demonstrate the importance of infinite accuracy of initial conditions, we iterate T. After only one iteration, d, or the distance between $T(X_0)$ and $T(X_1)$, has doubled. Iterating again, we find that the distance between the two points, already twice its initial size, doubles again. In this pattern, we find that the distance between the two points, $T^n(X_0)$ and $T^n(X_1)$, is $2^n d$. Clearly, d is expanding quite rapidly, leading the model further and further astray. After only ten iterations, the distance between the two points has grown to a whopping $2^{10}d = 1024d$.

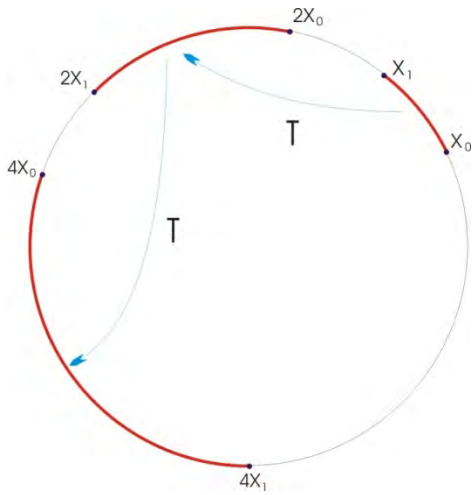

Figure 2.1 Mathematical roots of sensitive dependence

The example given above demonstrates that no matter how close two conditions start out, after only a few iterations, minor differences will be blown way out of proportion. The two points will separate from each other at an exponential rate. For a more relative example, we'll explore what happens when a computer conducts the same experiment with the circle. The particular point on the circle can only be specified with a finite number of decimal places, and the remaining decimal places are simple discarded. This means that even if the initial numbers are entered into the computer with precision, there will still be a certain amount of decimal error. After iterating, we quickly notice that the very small error is magnified so that the computed location of the point is actually very far away from the actual location of the point. A very tiny error in the initial conditions makes a very large difference in the outcome.

After discussing sensitive dependence, we are ready to summarize the qualities of a chaotic system. A chaotic system has these simple defining features:

- Chaotic systems are deterministic. This means they have some determining equation ruling their behavior.
- Chaotic systems are sensitive to initial conditions. Even a very slight change in the starting point can lead to significant different outcomes.
- Chaotic systems are not random, nor disorderly. Truly random systems are not chaotic; chaos has a sense of order and patter.

A function fR -> R exhibits deterministic chaos if it satisfies three properties

- Sensitive to initial conditions
  - Arbitrarily close to every point x, there is a point y with $f^n(x)$ and $f^n(y)$ iterating far apart
- Dense periodic points

  - Arbitrarily close to every point x, there is a point y with $f^m(y)=y$ for some m
- Mixing
  - For every pair of intervals I and J, for some k, $f^k(J)$ and I overlap

Critical Points

Mathematically, a critical point (or critical number) is defined as a point in the function's domain where the derivative is equal to zero or does not exist: that is, either a stationary point or a non-differentiable point.

Generalizing, there are two distinct concepts: either the derivative (Jacobian) vanishes, or it is not of full rank (that is the function in not differentiable); the value a function takes at a critical point is called a critical value ("points" are inputs, "values" are outputs). Elements of the function's range that are not critical values are called regular values.

The term "critical point" is often confused with "stationary point". Critical point has a broader meaning, it is either a stationary point or the derivative is undefined there.

When the function is smooth, the two are interchangeable, hence the confusion; when a function is understood to be smooth; all critical points are stationary points, but if the function has points of non-differentiability, one should distinguish these notions.

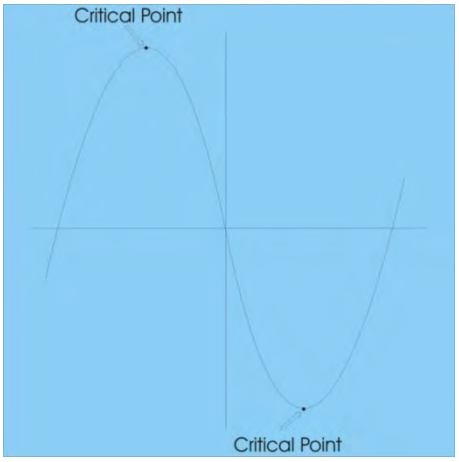

Figure 2.2 Graphic with two critical points

2.3 DYNAMICAL SYSTEMS

In a dynamical system we observe the world as a function of time. We express our observations as numbers and record how they change with time; given sufficiently detailed

information and understanding of the underlying natural laws, we see the future in the present as in a mirror. The motion of planets against the celestial firmament provides an example. Against the daily motion of the stars from East to West, the planets distinguish themselves by moving among the fixed stars. Ancients discovered that by knowing a sequence of planet's positions - latitudes and longitudes – its future position could be predicted quite accurately.

For the solar system, tracking the latitude and the longitude in the celestial sphere suffices to completely specify the planet's apparent motion. All possible values for positions and velocities of the planets form the phase space of the system. More generally, a state of a physical system, at a given instant in time, can be represented by a single point in an abstract space called state space or phase space $\mathcal{M}$. As the system changes, so does the representative point in state space. We refer to the evolution in time of such points as dynamics, and the function f(t) which specifies where the representative point is at time t as the evolution rule.

If there is a definite rule *f* that tells us how this representative point moves in $\mathcal{M}$, the system is said to be deterministic. For a deterministic dynamical system, the evolution rule takes one point of the state space and maps it into exactly one point. However, this is not always possible. For example, knowing the temperature today is not enough to predict the temperature tomorrow; knowing today's the stock value will not be enough determine its value tomorrow. The state space can be enlarged, in the hope that in a sufficiently large state space will enable us to determine an evolution rule; we imagine thus, that knowing the state of the atmosphere, measured on many points over the entire planet should be sufficient to determine the temperature tomorrow. Speaking of the climate, this is not quite enough; when it comes to stocks we are further away.

For a deterministic system almost every point has a unique future, so trajectories cannot intersect. We say "almost" because a set of measure zero (tips of wedges, cusps, etc.) may exist for which a trajectory is not defined. We may think of such sets as a nuisance, but it is quite the contrary, they will enable us to partition the state space, to better understand the dynamics.

Locally, the state space $\mathcal{M}$ looks like $\mathbb{R}^d$, meaning that *d* numbers are sufficient to determine what will happen next. Globally, it may be a more complicated manifold formed by patching together several pieces of $\mathbb{R}^d$, forming a torus, a cylinder, or some other geometric object. When we need to stress that, the dimension *d* of $\mathcal{M}$ is greater than one, we may refer to the point $x \in \mathcal{M}$ as x_i where $i = 1, 2, 3, \ldots,$ d. The evolution rule $f^t : \mathcal{M} \to \mathcal{M}$ tells us where a point *x* is in $\mathcal{M}$ after a time interval *t*. The pair $(\mathcal{M}, f)$ constitutes a dynamical system.

The dynamical systems we will study are smooth. This is expressed mathematically by saying that the evolution rule f^t can be differentiated as many times as needed. Its action on a point *x* is sometimes indicated by $f(x, t)$ to remind us that *f* is really a function of two variables: time and a point in state space. Note that time is relative rather than absolute, so only time intervals are necessary. This follows from the fact that a point in state space completely

determines all future evolution, and it is not necessary to know anything else. The time parameter can be a real variable ($t \in \mathbb{R}$), in which case the evolution is called a flow, or an integer ($t \in \mathbb{Z}$), in which case the evolution advances in discrete steps in time, given by iteration of a map. Actually, the evolution parameter need not be the physical time; for example, a time-stationary solution of a partial differential equation is parameterized by spatial variables. In such situations one talks of a "spatial profile" rather than a "flow".

Nature provides us with innumerable dynamical systems. They manifest themselves through their trajectories: given an initial point x_0, the evolution rule traces out a sequence of points $x(t) = f^t(x_0)$, the trajectory through the point $x_0 = x(0)$. A trajectory is parameterized by the time t and thus belongs to $(f^t(x_0), t) \in \mathcal{M} \times \mathbb{R}$. By extension, we can also talk of the evolution of a region $\mathcal{M}_i$ of the state space: just apply ft to every point in $\mathcal{M}_i$ to obtain a new region $f^t(\mathcal{M}_i)$, as in figure 2.8.

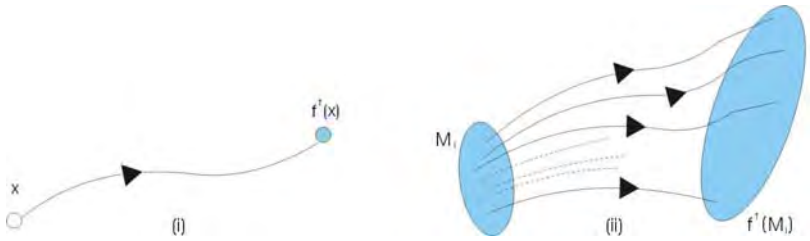

Figure 2.3 Trajectories traced by the evolution rule f^t. (i) Starting from a singled point x. (ii) Mapping a region $\mathcal{M}_i$.

Because f^t is a single-valued function, any point of the trajectory can be used to label the trajectory. If we mark the trajectory by its initial point x_0, we are using Lagrangian coordinates to describe it. We can regard the transport of a material point $x(0)$ at $t = 0$ to its current point $x(t) = f^t(x_0)$ as a coordinate transformation from Lagrangian coordinates to Eulerian coordinates.

The subset of points in $\mathcal{M}$ that belong to the (possibly infinite) trajectory of a given point x_0 is called the orbit of x_0. For a flow, an orbit is a smooth continuous curve; for a map, it is a sequence of points.

What are the possible trajectories? To which many answers can be given. Here is an attempt to classify all possible trajectories:

- stationary $f^t(x) = x$ for all t
- periodic $f^t(x) = f^{t+T_p}(x)$ for a given minimum period T_p
- aperiodic $f^t(x) \neq f^{t'}(x)$ for all $t \neq t'$.

The ancients tried to make sense of all dynamics in terms of periodic motions; epicycles, integrable systems. The embarrassing truth is that for a generic dynamical system almost all

motions are aperiodic. So we refine the classification by dividing aperiodic motions into two subtypes: those that wander off, and those that keep coming back.

A point $x \in \mathcal{M}$ is called a wandering point, if an open neighborhood $\mathcal{M}_0$ of x to which the trajectory never returns, exists.

$$f^t(x) \notin \mathcal{M}_0 \text{ for all } t > t_{\min} \tag{2.1}$$

In physics literature, the dynamics of such state is often referred to as transient.

A periodic orbit (or a cycle) corresponds to a trajectory that returns exactly to the initial point in a finite time. Periodic orbits form a very small subset of the state space, in the same sense that rational numbers are a set of zero measure on the unit interval.

Periodic orbits and stationary points are the simplest examples of "nonwandering" invariant sets preserved by dynamics. Dynamics can also preserve higher-dimensional smooth compact invariant manifolds; most commonly encountered are the M-dimensional tori of Hamiltonian dynamics, thus, generalizing periodic motion to quasiperiodic (superposition of M incommensurate frequencies) motion on a smooth torus.

For times much longer than a typical "turnover" time, it makes sense to relax the notion of exact (quasi)periodicity, and replace it by the notion of recurrence. A point is recurrent or non-wandering if for any open neighborhood $\mathcal{M}_0$ of x and any time $t_{\min}$ there exists a later time t, such that

$$f^t(x) \in \mathcal{M}_0 \,. \tag{2.2}$$

In other words, the trajectory of a non-wandering point reenters the neighborhood $\mathcal{M}_0$ infinitely often. We shall denote by Ω the non–wandering set of f, i.e., the union of all the non-wandering points of $\mathcal{M}$. The set Ω, the non–wandering set of f, is the key to understanding the long-time behavior of a dynamical system; all calculations undertaken here will be carried out on non–wandering sets.

So much about individual trajectories! What about clouds of initial points? If a connected state space volume exists that maps into itself under forward evolution (it can be proven by the method of Lyapunov functionals, or several other methods available in the literature), then the flow is globally contracting onto a subset of $\mathcal{M}$ which we shall refer to as the attractor. The attractor may be unique, or any number of distinct attracting sets, each with its own basin of attraction (the set of all points that fall into the attractor under forward evolution) can coexist. The attractor can be a fixed point, a periodic or an aperiodic orbit, or any combination of the above. The most interesting case is that of an aperiodic recurrent attractor, to which we shall refer loosely as a strange attractor. We say 'loosely', as will soon become apparent that diagnosing and proving existence of a genuine, card-carrying strange attractor is a highly nontrivial undertaking.

2.4 ATRACTORS AND BIFURCATIONS

Attractors

An attractor is a set of states (points in the phase space), invariant under the dynamics, toward which neighboring states (in) for a given basin of attraction asymptotically approach in the course of dynamic evolution. An attractor is defined as the smallest unit which cannot be decomposed into two or more attractors with distinct basins of attraction. This restriction is necessary since a dynamical system may have multiple attractors, each with its own basin of attraction.

Conservative systems do not have attractors, since the motion is periodic. For dissipative dynamical systems, however, volumes shrink exponentially so attractors have no volume in *n*-dimensional phase space.

We can identify four basic different types of attractors

Single Fixed Point Attractor

A single fixed point is a point that a system evolves towards, such as the final states of a falling pebble, a damped pendulum, or the water in a glass. It corresponds to a fixed point of the evolution function that is also attracting.

Periodic Attractor (Limit cycle)

A limit cycle is a periodic orbit of the system that is isolated. Examples include the swings of a pendulum clock, the tuning circuit of a radio, and the heartbeat while resting. The ideal pendulum is not an example because its orbits are not isolated. In phase space of the ideal pendulum, near any point of a periodic orbit there is another point that belongs to a different periodic orbit.

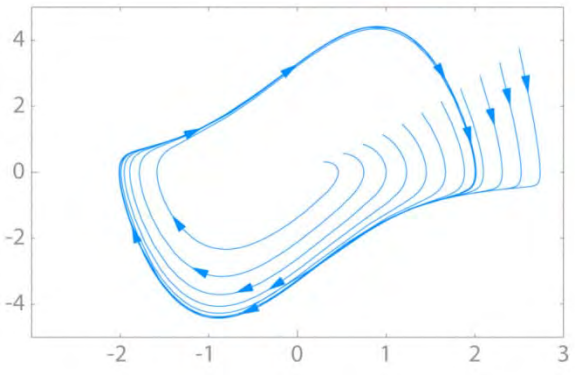

Figure 2.4 Van de Pol phase portrait

Limit Torus Attractor

There may be more than one frequency in the periodic trajectory of the system through the state of a limit cycle. If two of these frequencies form an irrational fraction (i.e. they are incommensurate), the trajectory will no longer be closed, and the limit cycle becomes a limit torus. We call this kind of attractor N_t-torus if there are N_t incommensurate frequencies.

A time series corresponding to this attractor is a quasiperiodic series: A discretely sampled sum of N_t periodic functions (not necessarily sine waves) with incommensurate frequencies. Such a time series does no longer have a strict periodicity, but its power spectrum still consists only of sharp lines.

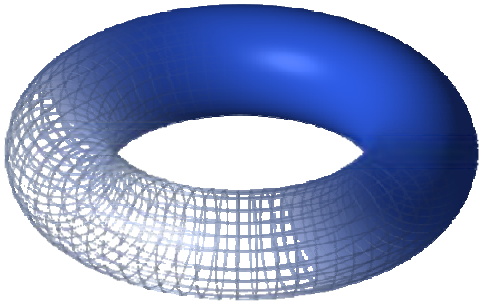

Figure 2.5 A simple 2-torus with a fading part

Strange Attractors

A strange attractor is the limit set of a chaotic trajectory. A strange attractor is an attractor that is topologically distinct from a periodic orbit or a limit cycle. It can also be considered a fractal attractor.

Consider a volume in phase space defined by all the initial conditions a system may have. For a dissipative system, this volume will shrink as the system evolves in time. If the system is sensitive to initial conditions, the trajectories of the points defining the initial conditions will move apart in some directions, closer in others, but there will be a net shrinkage in volume. Ultimately, all points will lie along a fine line of zero volume. This is the strange attractor. All initial points in phase space which ultimately land on the attractor form a Basin of Attraction. A strange attractor is obtained when a system is sensitive to initial conditions and is not conservative.

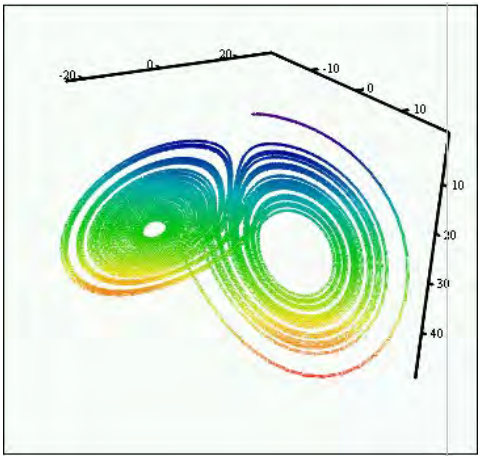

Figure 2.6 3-d visualization of Lorenz Attractor

Bifurcations

In the study of dynamical systems, a bifurcation occurs when a small smooth change made to the parameter values (the bifurcation parameters) of a system causes a sudden 'qualitative' or topological change in the system's long-term dynamical behavior. Bifurcations occur in both continuous systems (described by ODEs, DDEs or PDEs), and discrete systems (described by maps).

It is useful to divide bifurcations into two principal classes:

- Local bifurcations
- Global bifurcations

Local bifurcations

A local bifurcation occurs when a parameter change causes a change in the stability of an equilibrium or fixed point. In continuous systems, this corresponds to the real part of an eigenvalue of an equilibrium passing through zero. In discrete systems (those described by maps rather than ODEs), this corresponds to a fixed point having a Floquet multiplier with modulus equal to one. In both cases, the equilibrium is non-hyperbolic at the bifurcation point. The topological changes in the phase portrait of the system can be confined to arbitrarily small neighborhoods of the bifurcating fixed points by moving the bifurcation parameter close to the bifurcation point.

As an example we can take a period doubling bifurcation, in which the system switches to a new behavior with twice the period of the original system.

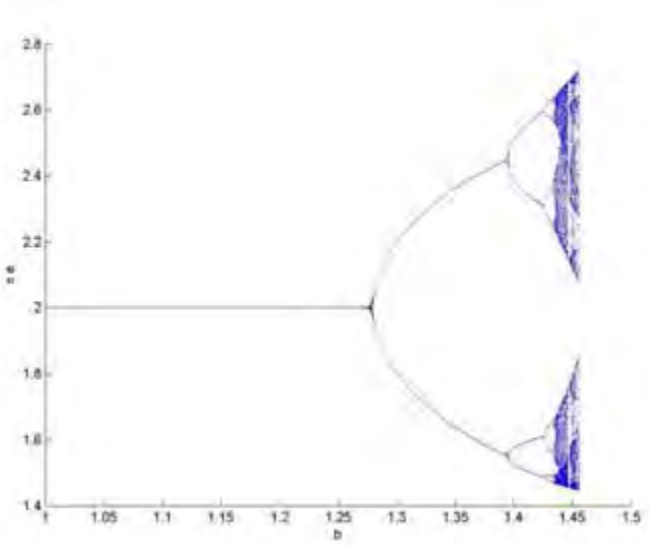

Figure 2.7 Bifurcation diagram for a modified Phillips curve. Period doubling bifurcation

Global Bifurcations

Global bifurcations occur when 'larger' invariant sets, such as periodic orbits, collide with equilibrium. This causes changes in the topology of the trajectories in the phase space which cannot be confined to a small neighborhood, as is the case with local bifurcations. In fact, the changes in topology extend out to an arbitrarily large distance.

As the simplest example of global bifurcations we present the homoclinic bifurcation in which a limit cycle collides with a saddle point.

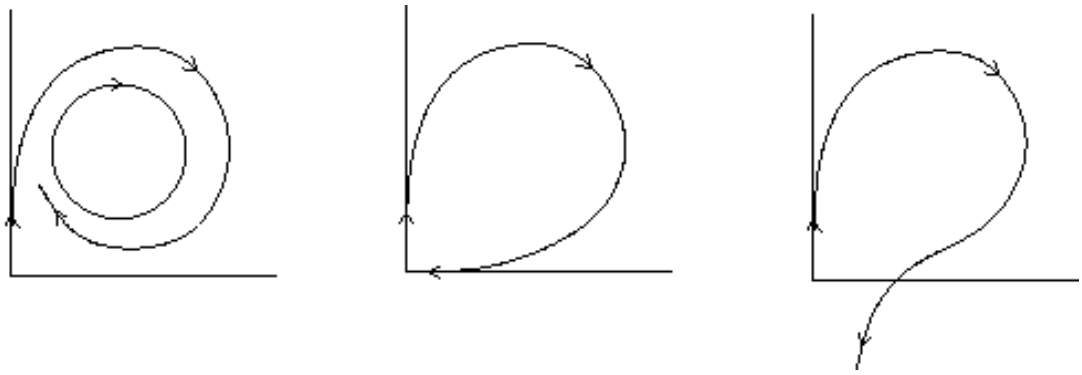

Figure 2.8 Phase portrait before, at, and after a monoclinic bifurcation in 2D

2.5 POINCARÉ SECTIONS

The time parameter in the sect. 2.3 definition of a dynamical system can be either continuous or discrete. Discrete time dynamical systems arise naturally from flows; one can observe the flow at fixed time intervals (by strobing it), or one can record the coordinates of the flow when a special event happens (the Poincaré section method). This triggering event can be as simple as a coordinate vanishing, or as complicated as the flow cutting through a curved hypersurface.

Successive trajectory intersections with a Poincaré section, a *d*-dimensional hypersurface or a set of hypersurfaces $\mathcal{P}$ embedded in the (*d*+1)-dimensional state space $\mathcal{M}$, define the Poincaré return map P(*x*), a *d*-dimensional map of form

$$x' = P(x) = f^{\tau(x)}(x)\,, \qquad x', x \in \mathcal{P}\,. \tag{2.3}$$

For economy of notation, the maps of this chapter will be taken to be *d*-dimensional and the associated flows (*d*+1)-dimensional). Here the first return function τ(*x*) - sometimes referred to as the ceiling function - is the time of flight to the next section for a trajectory starting at *x*. The choice of the section hypersurface $\mathcal{P}$ is altogether arbitrary. It is rarely possible to define a single section that cuts across all trajectories. In practice one often needs only a local section - a finite hypersurface of codimension 1 intersected by a ray of trajectories near the trajectory of interest. The hypersurface can be specified implicitly through a function U(*x*) that is zero whenever a point *x* is on the Poincaré section,

$$x \in \mathcal{P} \text{ iff } U(x)\,. \tag{2.4}$$

The gradient of U(*x*) evaluated at $x \in \mathcal{P}$ serves a two-fold function. First, the flow should pierce the hypersurface $\mathcal{P}$, rather than be tangent to it. A nearby point $x + \delta x$ is in the hypersurface $\mathcal{P}$ if $U(x + \delta x) = 0$. A nearby point on the trajectory is given by $\delta x = v\delta t$, so a traversal is ensured by the transversality condition

$$(v\cdot\partial U) - \sum_{j=1}^{d+1} v_j(x)\partial_j U(x) \neq 0\,, \quad \partial_j U(x) - \frac{d}{dx_j}U(x)\,, \quad x \in \mathcal{P} \tag{2.5}$$

Second, the gradient $\partial_j U$ defines the orientation of the hypersurface $\mathcal{P}$. The flow is oriented as well, and a periodic orbit can pierce $\mathcal{P}$ twice, crossing it in both directions, as in figure 2.9. Hence the definition of Poincaré return map P(*x*) needs to be supplemented with the orientation condition

$$x_{n+1} = P(x_n)\,, \qquad U(x_{n+1}) = U(x_n) = 0\,, \quad n \in \mathbb{Z}^+$$
$$\sum_{j=1}^{d+1} v_j(x_n)\partial_j U(x_n) > 0\,. \tag{2.6}$$

In this way the continuous time t flow $f^t(x)$ is reduced to a discrete time n sequence x_n of successive oriented trajectory traversals of ℙ.

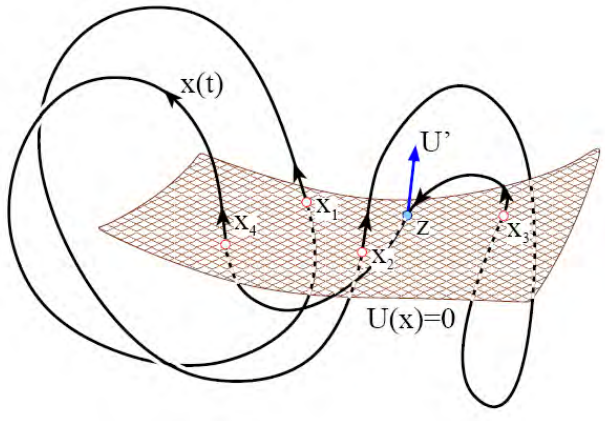

Figure 2.9 An $x(t)$ trajectory that intersects a Poincaré section ℙ at four different times

With a sufficiently clever choice of a Poincaré section or a set of sections, any orbit of interest will intersect a section. Depending on the application, one might need to convert the discrete time n back to the continuous flow time. This is accomplished by adding up the first return function times $\tau(x_n)$, with the accumulated flight time given by

$$t_{n+1} = t_n + \tau(x_n), \qquad t_0 = 0, \qquad xn \in \mathbb{P}\,. \tag{2.7}$$

2.6 SECOND CHAPTER REFERENCES

- J.M. THOMPSON, **NONLINEAR DYNAMICS AND CHAOS**, John Wiley & Sons, 1986
- J. CHANDRA, **CHAOS IN NONLINEAR DYNAMICAL SYSTEMS**, Siam, 1984
- W. J.F. GOVAERTS, **NUMERICAL METHODS FOR BIFURCATIONS OF DYNAMICAL EQUILIBRIA**, Siam, 1990
- P. CVITANOVIC & CO., **CHAOS, CLASSICAL AND QUANTUM**, MIR, 2006
- K.T. ALLIGOOD & CO., **CHAOS: AN INTRODUCTION TO DYNAMICAL SYSTEMS**, Springer, 1996

CHAPTER 3

3.1 INTRODUCTION

In this chapter, the rate equations in the general form proposed by H. Statz and G. de Mars in 1960[1] will be approached and their physical interpretation discussed, these equations are independent of the number of levels involved on the laser system. We will consider a brief introduction to saturable absorbers because of their crucial importance in the realization of this work; after that, the laser model of our principal study will be presented and a stability analysis of the Statz-de Mars equations made, in order to determine the regions of stability and chaos in our dynamical laser system.

3.2 STATZ- DE MARS EQUATIONS

In section 1.10 we obtained a rate equations system (1.47) and (1.48) to describe a laser system with two energy levels, an innocent question pops up; how can we make a model for a laser system with more energy levels? In 1960 H. Statz and G. de Mars obtained a generalized form of the rate equations, independent of the number of energy levels involved in the laser to be modeled. This phenomenological model is expressed by the following equations:

$$\frac{dM}{dt} = B'M(t)N(t) - \frac{M(t)}{T} \tag{3.1}$$

$$\frac{dN}{dt} = \beta B'M(t)N(t) + \frac{N_0 - N(t)}{\tau} \tag{3.2}$$

where N(t) represents the population inversion density and M(t) the emitted photon density at a determinate frequency. The emitted photon density is directly linked with the photon-flux density S(t). If we divide the photon-flux between the propagation speed of light **v** and the photons energy hν we obtain the emitted photons density; this is:

$$M(t) = \frac{S(t)}{\mathrm{v}h\nu} \tag{3.3}$$

In this section, the constant B' would mean Bhν, where B is the Einstein coefficient for stimulated transitions. T represents the photons lifetime inside the resonant cavity, which happens to be inversely proportional to the sum of the losses coefficients ξ_1 and ξ_2:

$$T = \frac{1}{\mathrm{v}(\xi_1 + \xi_2)} \tag{3.4}$$

τ represents the relaxation time of the population inversion difference between levels where the laser emission takes place; β is a constant that depends of the level numbers of the system and N_0 represents the equilibrium value of the population inversion density achieved in absence of laser oscillation.

The physical interpretation of the Statz-de Mars equations is especially simple. The first equation means that the photons density grows as a consequence of the stimulated transitions inside the cavity and decreases because of the losses imputable to the medium. The growth of the emitted photons density to a certain frequency is directly proportional to the product of the same emitted photons quantity at that frequency by the population inversion density of the laser medium. The second equation shows that the population inversion density will decrease because of the stimulated emission and will grow by the pumping action on the upper energy levels of the medium.

To achieve laser emission is necessary for the population inversion density to reach a critical value N_c. We can find this value under the steady state condition (dM/dt > 0); equation (3.1) gives:

$$B'N(t) - {}^{1}/_{T} > 0 \tag{3.5}$$

$$N(t) > {}^{1}/_{B'T} \tag{3.6}$$

And therefore,

$$N_c = \frac{1}{B'T} = \frac{1}{Bh\nu T} = \frac{1}{BhQ} \tag{3.7}$$

Q being the quality factor of the cavity.

Moreover we have that σ = (Bhν)/**v** and T=1/v(ξ_1+ξ_2), therefore:

$$N_c = \frac{\xi 1+\xi 2}{\sigma} \tag{3.8}$$

Since population inversion cannot exceed the value N_0; In order to achieve laser oscillation the next condition must be fulfilled:

$$N_c < N < N_0 \tag{3.9}$$

For an easier management of the Statz-de Mars equations we define the following non dimensional parameters:

t' = t/τ	Adimensional time
m(t') = βB' τM(t', τ)	Field intensity
n(t') = N(t', τ)/N_c	Population inversion density
α = B'TN_0/N_c	Pumping parameter

G = τ/T	Relaxation time relation with the photons lifetime inside the cavity

With these new parameters the Statz – de Mars equations are expressed as follows:

$$\frac{dm}{dt'} = Gm(n-1) \tag{3.10}$$

$$\frac{dn}{dt'} = \alpha - n(m+1) \tag{3.11}$$

3.3 SATURABLE FILTERS

Saturable absorption is a property some materials present, where light absorption decreases as its intensity is increased. Although most materials show some saturable absorption, often it is only at very high optical intensities.

A saturable absorber is an optical component with a certain optical loss, which is reduced for high optical intensities. This usually happens in a medium doped with absorbing ions, as a strong optical intensity leads then to the depletion of the ions ground state. Similar effects can occur in semiconductors.

Saturable absorbers are widely used in passive mode locking and Q switching of lasers, i.e., for short pulses generation. However, one can also use saturable absorbers for purposes of nonlinear filtering outside of laser resonators, e.g. for cleaning up pulse shapes, and in optical signal processing.

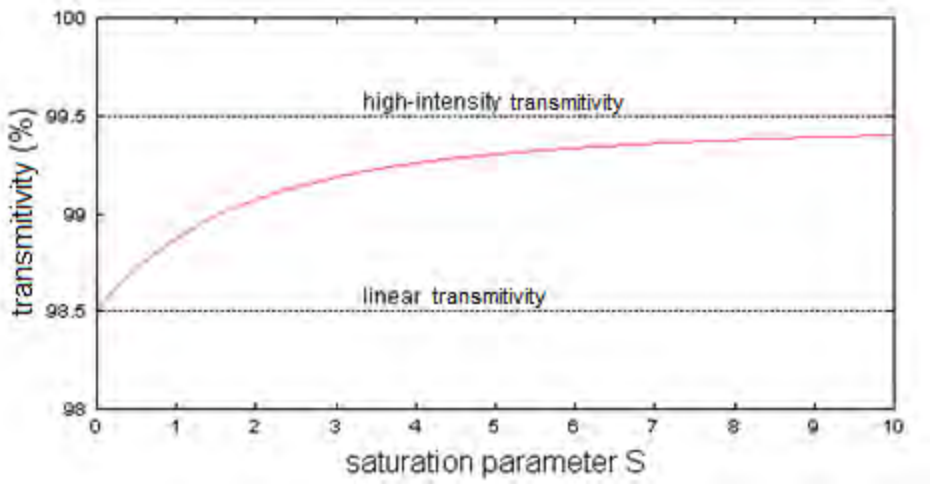

Figure 3.1 Transmitivity of a slow saturable absorber vs. saturation parameter (S), which is the pulse fluence divided by the saturation fluence of the device. The modulation depth (maximum change of transmitivity) is 1%, and the nonsaturable losses are 0.5%.

Types of Saturable Absorbers (Q-switches)

Since different applications require saturable absorbers with very different parameters, rather different materials and techniques are used:

- For passive Q switching of solid state lasers, Cr4+:YAG and V3+:YAG crystals are the most popular. (They are actually also used as gain media → chromium-doped gain media.)
- Particularly for passive mode locking (but also for Q switching), semiconductor saturable absorber mirrors (also called SESAMs) are frequently used.
- Other semiconductor saturable absorbers for mode locking are based on quantum dots e.g. of lead sulfide (PbS) suspended in glasses.
- In rare cases, saturable absorber materials are used as optical fibers. For example, chromium, samarium or bismuth dopants can serve this function in Q-switched fiber lasers.
- Avly saturable absorbers were dyes such as Rh6G

Artificial Saturable Q-Switches

There are also many artificial Q-switches. These devices exhibit decreasing optical losses for higher intensities, but do not actually exploiting saturable absorption. Such devices can be based on any of the following:

- Kerr lenses combined with some kind of aperture (→ Kerr lens mode locking).
- Nonlinear polarization rotation in a fiber, combined with a polarizing element, often used for passive mode locking of fiber lasers.
- A nonlinear fiber loop mirror, also often used for mode locking.
- A nonlinear mirror device containing a frequency-doubling crystal, as sometimes used for passive mode locking of solid state bulk lasers.

The most important characteristics of saturable absorbers are:

- modulation depth, i.e., the optical loss maximum possible change
- unsaturable losses, i.e., the (typically unwanted) part of the losses which cannot be saturated
- recovery time, i.e., the decay time of the excitation after an exciting pulse
- saturation fluence, i.e., the fluence (energy per unit area) necessary to reduce the initial value to 1/e (≈37%) of its initial value
- saturation energy, is the saturation fluence times the mode area

- saturation intensity, i.e., optical intensity (power per unit area) to enable the absorption reduction of a steady-state to one half its unbleached value
- saturation power is the saturation intensity times the mode area
- damage threshold (in terms of an intensity or fluence)

When dealing with pulses, a fast saturable absorber has a recovery time well below the pulse duration, while a slow absorber has it well above the pulse duration. The same device may be either a fast absorber or a slow absorber, depending on the pulses used with.

The saturation parameter of a saturable absorber is the ratio of the incident pulse fluence to the saturation fluence of the device.

3.4 LASER MODEL

We suppose a three level laser obeying the following equations:

$$\frac{1}{\mathrm{v}}\frac{dS(t)}{dt} = \sigma N(t)S(t) - (\xi_1 + \xi_2)S(t) \tag{3.12}$$

$$\frac{dN(t)}{dt} = -\frac{2\sigma}{h\omega}S(t)N(t) - (Z+1)\frac{N(t)}{\tau} + (Z-1)\frac{n}{\tau} \tag{3.13}$$

where:

S(t) is the photon-flux density inside the cavity

N(t) is the population inversion density inside the cavity

σ is the effective cross section of interaction between active centers and photons

ξ_1 coefficient due to absorption and dispersion

ξ_2 coefficient taking care of the losses dependence on the mirrors reflectivity

v speed of light in the medium

τ lifetime between energy levels

n number of active centers per volume unit on the medium

$Z=W_p\tau$ where W_p is the stimulated emission transition probability

The saturable absorber will be modeled by two-level active resonant centers, so that all the active absorbents centers are on a lower energy level to get the resonant photons to cause the maximum opacity. The rate equations that describe the active centers of the absorber are:

$$\frac{dn_{2\alpha}}{dt} = \mathrm{B}_{\alpha} n_{1\alpha} \frac{S}{\mathrm{v}_{\alpha}} - \mathrm{B}_{\alpha} n_{2\alpha} \frac{S}{\mathrm{v}_{\alpha}} - \frac{n_{2\alpha}}{\tau_{\alpha}} \tag{3.14}$$

$$\frac{dn_{1\alpha}}{dt} = \mathrm{B}_{\alpha} n_{2\alpha} \frac{S}{\mathrm{v}_{\alpha}} - \mathrm{B}_{\alpha} n_{1\alpha} \frac{S}{\mathrm{v}_{\alpha}} - \frac{n_{2\alpha}}{\tau_{\alpha}} \tag{3.15}$$

where B_{α} is the Einstein coefficient for stimulated emission on the absorber, and $\frac{1}{\tau_{\alpha}}$ is the probability of spontaneous emission for the absorbers active centers. Denoting by n_{1a} and n_{2a} the density of active centers of the absorber in the lower and upper energy levels, respectively, the total density of active centers of the absorber is given by $n_{\alpha} = n_{1\alpha} + n_{2\alpha}$ and then we have that t = 0:

$$n_{1\alpha} = n_{\alpha} \tag{3.16}$$

$$n_{2\alpha} = 0 \tag{3.17}$$

when we apply enough power pump we can reach the saturation condition described by:

$$n_{1\alpha} = n_{2\alpha} = \frac{n_{\alpha}}{2} \tag{3.18}$$

Population inversion density of the absorber is defined as $N_{\alpha} = n_{2\alpha} - n_{1\alpha}$, deducing from equations (3.17) and (3.18) we have

$$\frac{dN_{\alpha}}{dt} = -\frac{2B_{\alpha} N_{\alpha} S}{\mathrm{v}_{\alpha}} - \frac{\left(N_{\alpha} + n_{\alpha}\right)}{\tau_{\alpha}} \tag{3.19}$$

Defining the absorption coefficient for the absorber as:

$$k_{\alpha} = -\sigma_{\alpha} N_{\alpha} \tag{3.20}$$

where σ_{α} is the effective section of stimulated emission given by:

$$\sigma_{\alpha} = \frac{\hbar \omega B_{\alpha}}{\mathrm{v}_{\alpha}} \tag{3.21}$$

where v_{α} represents the speed of light on the absorber and ω is the angular frequency.

If we multiply equation (3.19) by $-\sigma_{\alpha}$, it can be rewritten as:

$$\frac{dk_{\alpha}}{dt} = -\frac{2B_{\alpha} k_{\alpha} S}{\mathrm{v}_{\alpha}} + \frac{\left(k_{0\alpha} - k_{\alpha}\right)}{\tau_{\alpha}} \tag{3.22}$$

where $k_{0\alpha}$ is the initial absorption coefficient $k_{0\alpha} = -\sigma_\alpha N_\alpha(0) = \sigma_\alpha n_\alpha$.

steady-state implies that $\frac{dk_\alpha}{dt} = 0$, and equation (3.22) becomes:

$$k_\alpha = \frac{k_{0\alpha}}{1 + \frac{S}{S_{\alpha_{Sat}}}} \tag{3.23}$$

where $S_{\alpha_{Sat}}$ is the photon-flux in where the absorption coefficient k_α falls down to half its initial value $k_{0\alpha}$.

Being ξ_α the non-resonant absorption coefficient and K_α the total absorption coefficient of the absorber:

$$K_\alpha = k_\alpha + \xi_\alpha \tag{3.24}$$

Is satisfied, and the photon-flux average equation of the active medium may be expressed by:

$$S_{S\alpha t} + \frac{L_m}{v}\frac{d\langle S\rangle}{dt} = L_m\sigma\langle N\rangle\langle S\rangle - L_m(\xi_1)\langle S\rangle \tag{3.25}$$

where L_m is the active medium length.

The photon-flux average equation inside the absorber is given by:

$$S_{S\alpha t} + \left(\frac{L_m}{v} + \frac{L_\alpha}{v_\alpha} + \frac{L-(L_m+L_\alpha)}{c}\right)\frac{d\langle S\rangle}{dt} = L_m\sigma\langle N\rangle\langle S\rangle + L_\alpha\sigma_\alpha\langle N_\alpha\rangle\langle S\rangle - L_m\xi_l\langle S\rangle - L_\alpha\xi_\alpha\langle S\rangle \tag{3.26}$$

And the fill coefficient of the cavity as:

$$\Gamma = \frac{L_m n}{L_m n + L_\alpha n_\alpha + [L-(L_m+L_\alpha)]} = \frac{\frac{L_m}{v}}{\frac{L_m}{v} + \frac{L_\alpha}{v_\alpha} + \frac{[L-(L_m+L_\alpha)]}{c}} \tag{3.27}$$

where $n = \frac{c}{\mathrm{v}}$ and $n_\alpha = \frac{c}{\mathrm{v}_\alpha}$ are the refractive index on the active medium and inside the absorber, respectively, L is the cavity length and L_α the saturable absorber length. Because $S_{S\alpha t} = L_m(S)(\xi_2)$, equation (3.26) becomes then:

$$\frac{1}{\Gamma \mathrm{v}}\frac{dS}{dt} = \left(\sigma N + \frac{L_\alpha}{L_m}\sigma_\alpha N_\alpha\right)S - \left(\xi_1 + \xi_2 + \frac{L_\alpha}{L_m}\xi_\alpha\right)S \tag{3.28}$$

This is the photon-flux equation inside a cavity with an active medium and a saturable absorber, as shown in figure 3.2.

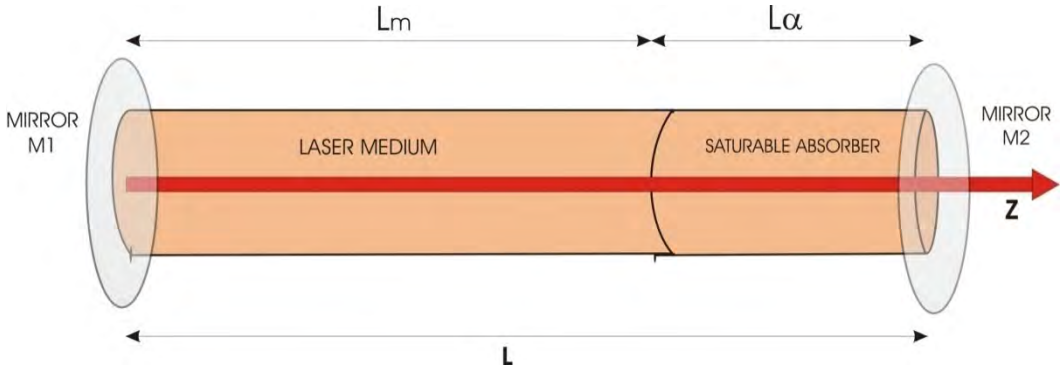

Figure 3.2 a laser cavity with an active medium and a saturable absorber.

given that $k_\alpha = -\sigma_\alpha N_\alpha$ and defining T as the photons lifetime inside a cavity with the form:

$$T = \frac{1}{\Gamma\left(\xi_1 + \xi_2 + \frac{L_\alpha}{L_m}\xi_\alpha\right)} \tag{3.29}$$

Using this equation, we can rewrite equation (3.28) as:

$$\frac{dS}{dt} = \Gamma v \sigma N S - \Gamma v \frac{L_\alpha}{L_m} k_\alpha S - \frac{1}{T} S \tag{3.30}$$

Therefore, for a complete description of a laser with saturable absorber, time evolution, the only three equations that we need are: the photon-flux equation, an equation for the population inversion density on the active medium and last the saturable population inversion equation that gives us the saturation coefficient (taking into account $k_\alpha = -\sigma_\alpha N_\alpha$):

$$\frac{dS}{dt} = \Gamma v \sigma N S - \Gamma v \frac{L_\alpha}{L_m} k_\alpha S - \frac{1}{T} S \tag{3.31}$$

$$\frac{dN}{dt} = -\beta \frac{\sigma}{h\omega} N S + \frac{N_0 - N}{\tau} \tag{3.32}$$

$$\frac{dk_\alpha}{dt} = -\frac{2\sigma_\alpha k_\alpha S}{\hbar\omega} + \frac{k_{0\alpha} - k_\alpha}{\tau_\alpha} \tag{3.33}$$

If we define the follows non-dimensional parameters:

$$t' = t/\tau$$
$$G = \tau/T$$
$$\delta = \tau/\tau_\alpha$$
$$\rho = 2\sigma_\alpha/\beta\sigma$$
$$\alpha = \Gamma \mathrm{v}\sigma TN$$
$$\alpha_\alpha = -\Gamma \mathrm{v} T k_{0\alpha} L_\alpha / L_m = -\Gamma \mathrm{v} T \sigma_\alpha n_\alpha / L_m$$

and:

$$n(t') = \Gamma \mathrm{v}\sigma TN(t') \tag{3.34}$$

$$n_\alpha = -\Gamma \mathrm{v} T k_\alpha(t') \frac{L_\alpha}{L_m} \tag{3.35}$$

$$m(t') = \beta B \tau \frac{S(t')}{\mathrm{v}} = \beta\sigma\tau S(t')/h\omega \tag{3.36}$$

We can rewrite our equation system (3.31), (3.32) & (3.33) as follows:

$$\frac{dm}{dt'} = Gm(n + n_\alpha - 1) \tag{3.37}$$

$$\frac{dn}{dt'} = \alpha - n(m+1) \tag{3.38}$$

$$\frac{dn_\alpha}{dt'} = \alpha_\alpha \sigma - n_\alpha(\rho m + \delta) \tag{3.39}$$

These three differential equations compose our working system for this chapter, and results will be discussed at the end of this chapter and the next one. We will find the solution to our system.

3.5 STABILITY ANALISYS

The system critical points are obtained by the jacobian of the function (derivatives) and are the next ones:

$$\mathrm{Q}_1 = \left(0, \alpha, \frac{\alpha_\alpha \sigma}{\delta}\right) \tag{3.40}$$

$$\mathrm{Q}_2 = (\alpha - 1, 1, 0) \tag{3.41}$$

$$\mathrm{Q}_3 = \left(\frac{\alpha_\alpha \sigma - \delta}{\rho}, 0, 1\right) \tag{3.42}$$

The critical points will be used to make the stability analysis of the system; the analysis for each critical point is as follows:

First critical point Q_1

Due the result (3.40), for a simpler work we will make the next variable change:

$$\mathrm{m}(\mathrm{t}') = u(t') \tag{3.43}$$

$$\mathrm{n}(\mathrm{t}') = v(t') + \alpha \tag{3.44}$$

$$\mathrm{n}_{\alpha}(\mathrm{t}') = w(t') + \alpha_{\alpha} \tag{3.45}$$

And then, we can rewrite our system as follows:

$$\frac{\mathrm{d}u}{\mathrm{d}t'} = Gu\left(v + \alpha + w + \alpha_{\alpha} - 1\right) \tag{3.46}$$

$$\frac{\mathrm{d}v}{\mathrm{d}t'} = \alpha - \left(v + \alpha\right)\left(u + 1\right) \tag{3.47}$$

$$\frac{\mathrm{d}w}{\mathrm{d}t'} = \alpha_{\alpha}\sigma - \left(w + \alpha_{\alpha}\right)\left(\rho u + \delta\right) \tag{3.48}$$

The fixed points of our new system called system A (eqs. 3.46, 3.47 & 3.48) are obtained from the systems steady-state condition:

$$Gu\left(v + \alpha + w + \alpha_{\alpha} - 1\right) = 0 \tag{3.49}$$

$$\alpha - \left(v + \alpha\right)\left(u + 1\right) = 0 \tag{3.50}$$

$$\alpha_{\alpha}\sigma - \left(w + \alpha_{\alpha}\right)\left(\rho u + \delta\right) = 0 \tag{3.51}$$

When the equations are solved we obtained the next information for m, n and n_{α}

$$m = \frac{\alpha + \alpha_{\alpha} - 1}{\alpha_{\alpha}\left(\rho - 1\right) + 1} \tag{3.52}$$

$$n = \frac{\alpha\left(\rho\alpha_{\alpha} - \alpha\right)}{\rho\alpha_{\alpha} + \alpha} \tag{3.53}$$

$$n_{\alpha} = \alpha_{\alpha} - \rho\alpha_{\alpha}\left(\frac{\rho\alpha_{\alpha} - \alpha}{\rho\alpha_{\alpha} + \alpha}\right) \tag{3.54}$$

If we evaluate this results with Q_1 we have:

$$\alpha_\alpha + \alpha = 1 \tag{3.55}$$

$$\rho\alpha_\alpha = \alpha \tag{3.56}$$

If we consider $w = 0$ in our system A, we can write it as:

$$\frac{\mathrm{d}u}{\mathrm{d}t'} = Gu(\alpha + \alpha_\alpha - 1) \tag{3.57}$$

$$\frac{\mathrm{d}v}{\mathrm{d}t'} = -\alpha u - v \tag{3.58}$$

And then, we have that its characteristic equation is:

$$\lambda^2 + \lambda + \alpha = 0$$

And its solution is:

$$\lambda_\pm = \frac{-1 \pm \sqrt{1-4\alpha}}{2} \tag{3.59}$$

Because the typical α values are comprised between 2 and 30, λ_1 and λ_2 are complex, in consequence we will have a stable spiral approaching.

If we consider $v = 0$ for the system A we will have:

$$\frac{\mathrm{d}u}{\mathrm{d}t'} = Gu(\alpha + \alpha_\alpha - 1) \tag{3.60}$$

$$\frac{\mathrm{d}w}{\mathrm{d}t'} = \alpha_\alpha\sigma - \delta w + \alpha_\alpha u \tag{3.61}$$

Therefore its characteristic equation is:

$$\lambda^2 + \delta\lambda = 0$$

And its solutions are:

$$\lambda_1 = 0 \tag{3.62}$$

$$\lambda_1 = -\delta \tag{3.63}$$

Because λ_1 is bigger than λ_2 and they are less or equal to zero, we will observe and approaching on the m, n_α plane like an instable node.

Considerating $u = 0$ we can rewrite our system A as follows:

$$\frac{\mathrm{d}v}{\mathrm{d}t'} = -v \tag{3.64}$$

$$\frac{\mathrm{d}w}{\mathrm{d}t'} = -\delta w \tag{3.65}$$

Therefore its characteristic equation is:

$$\lambda^2 + [1+\delta]\lambda + \delta = 0$$

And its solutions are:

$$\lambda_1 = -1 \tag{3.66}$$

$$\lambda_2 = -\delta \tag{3.67}$$

Because λ_1 is bigger than λ_2 and they are lesser than zero, we will observe and approaching on the n, n_α plane like an instable node.

Second Critical Point Q_2

Due to result (3.41), we propose the next changes of variables

$$\mathrm{m}(\mathrm{t}') = u(t') + \alpha - 1 \tag{3.68}$$

$$\mathrm{n}(\mathrm{t}') = v(t') + 1 \tag{3.69}$$

$$\mathrm{n}_\alpha(\mathrm{t}') = w(t') \tag{3.70}$$

With those changes our main system can be renamed as B and rewritten as:

$$\frac{\mathrm{d}u}{\mathrm{d}t'} = G(u + \alpha - 1)(v + w) \tag{3.71}$$

$$\frac{\mathrm{d}v}{\mathrm{d}t'} = \alpha - (v+1)(u+\alpha) \tag{3.72}$$

$$\frac{\mathrm{d}w}{\mathrm{d}t'} = \alpha_\alpha \delta - w(\rho(u + \alpha - 1) + \delta) \tag{3.73}$$

The fixed points for system B expressed with the m, n and n_α variables are:

$$m = \frac{\alpha\alpha_\alpha\delta}{\delta+\rho\alpha-\rho}+\alpha-1 \tag{3.74}$$

$$n = -\frac{\alpha_\alpha\delta}{\delta+\rho\alpha-\rho}+1 \tag{3.75}$$

$$n_\alpha = \frac{\alpha_\alpha\delta}{\delta+\rho\alpha-\rho} \tag{3.76}$$

If we evaluate those results with Q_2 we have:

$$\alpha_\alpha\sigma = 0 \tag{3.77}$$

Considerating $w = 0$ in our system B we can rewrite it as:

$$\frac{\mathrm{d}u}{\mathrm{d}t'} = Gv(\alpha-1) \tag{3.78}$$

$$\frac{\mathrm{d}v}{\mathrm{d}t'} = -u-\alpha v \tag{3.79}$$

And then, we have that its characteristic equation is:

$$\lambda^2+\alpha\lambda+G(\alpha-1)=0$$

Whose solutions are:

$$\lambda_\pm = \frac{-\alpha\pm\sqrt{\alpha^2-4(G(\alpha-1))}}{2} \tag{3.80}$$

Because the typical α values are comprised between 2 and 30 and the G values are between 10^2 and 10^5, λ_1 and λ_2 describe a stable spiral as they approach.

If we consider $v = 0$ system B can be rewritten as:

$$\frac{\mathrm{d}u}{\mathrm{d}t'} = Gw(\alpha-1) \tag{3.81}$$

$$\frac{\mathrm{d}w}{\mathrm{d}t'} = \alpha_\alpha\delta-w(\alpha\rho-\rho+\delta) \tag{3.82}$$

Its characteristic equation is:

$$-\lambda\left(-\left(\alpha\rho-\rho+\delta\right)-\lambda\right)=0$$

With solutions:

$$\lambda_1=0 \tag{3.83}$$

$$\lambda_2=-\left(\alpha\rho-\rho+\delta\right) \tag{3.84}$$

Since λ_1 is bigger than λ_2 and they are lesser or equals to zero, the node is an instable node approaching in the m, n_α plane.

If we make $u=0$ in our system B, we can rewrite it as:

$$\frac{\mathrm{d}v}{\mathrm{d}t'}=-\alpha v \tag{3.85}$$

$$\frac{\mathrm{d}w}{\mathrm{d}t'}=\alpha_\alpha\delta-w\left(\rho\left(\alpha-1\right)+\delta\right) \tag{3.86}$$

Its characteristic equation is:

$$\lambda^2-\left(\left(\rho\left(\alpha-1\right)+\delta\right)-\alpha\right)\lambda-\left(\rho\left(\alpha-1\right)+\delta\right)\alpha=0$$

And its solutions are:

$$\lambda_1=\alpha \tag{3.87}$$

$$\lambda_2=-\left(\rho\left(\alpha-1\right)+\delta\right) \tag{3.88}$$

Under these conditions we will observe an unstable chair approaching, because $\lambda_2<0<\lambda_1$.

Third Critical Point Q_3

For a simpler mathematical work and due the result (3.42) we propose the next change of variable:

$$\mathrm{m}\left(\mathrm{t}'\right)=u\left(t'\right)+\frac{\alpha_\alpha\delta-\delta}{\rho} \tag{3.89}$$

$$\mathrm{n}\left(\mathrm{t}'\right)=v\left(t'\right) \tag{3.90}$$

$$\mathrm{n}_\alpha\left(\mathrm{t}'\right)=w\left(t'\right)+1 \tag{3.91}$$

Our mainl equation system renamed as system C can be rewritten as follows:

$$\frac{\mathrm{d}u}{\mathrm{d}t'} = G(u+\alpha_\alpha)(v+w) \tag{3.92}$$

$$\frac{\mathrm{d}v}{\mathrm{d}t'} = \alpha - v(u+\alpha_\alpha+1) \tag{3.93}$$

$$\frac{\mathrm{d}w}{\mathrm{d}t'} = \alpha_\alpha\sigma - (w+1)(\rho(u+\alpha_\alpha)+\delta) \tag{3.94}$$

We found the fixed points for m, n and n_α as follows:

$$m = -\alpha_\alpha + \frac{\alpha_\alpha\delta}{\rho} - \frac{\delta}{\rho} \tag{3.95}$$

$$n = \alpha \tag{3.96}$$

$$n_\alpha = 1-\alpha \tag{3.97}$$

Evaluating those points for Q_3 we obtained:

$$\alpha = 0 \tag{3.98}$$

$$\alpha_\alpha\sigma = 0 \tag{3.99}$$

Considerating $w = 0$ in our system C we obtained the next equations:

$$\frac{\mathrm{d}u}{\mathrm{d}t'} = 0 \tag{3.100}$$

$$\frac{\mathrm{d}v}{\mathrm{d}t'} = -v \tag{3.101}$$

The characteristic equation being:

$$-\lambda(-1-\lambda) = 0$$

And its solutions are:

$$\lambda_1 = 0 \tag{3.102}$$

$$\lambda_2 = -1 \tag{3.103}$$

In this case the trajectory towards the point Q_3 is in the form of an unstable node.

Now as we consider $v = 0$ in our system C, we find the next equations:

$$\frac{du}{dt'} = 0 \tag{3.104}$$

$$\frac{dw}{dt'} = -\rho u - (w+1)(\delta) \tag{3.105}$$

With characteristic equation:

$$\lambda(\lambda - \delta) = 0$$

And solutions:

$$\lambda_1 = 0 \tag{3.106}$$

$$\lambda_2 = \delta \tag{3.107}$$

We observe that λ_1 is smaller than λ_2 and they are lesser or equals to zero, therefore we have an unstable chair approaching in the m, n_α plane.

Assuming $u = 0$ for our system C, we find the next equations:

$$\frac{dv}{dt'} = 0 \tag{3.108}$$

$$\frac{dw}{dt'} = w(\rho - \delta) \tag{3.109}$$

And its characteristic equation is:

$$\lambda(\rho - \delta - \lambda) = 0$$

In which case the solutions are:

$$\lambda_1 = 0 \tag{3.110}$$

$$\lambda_2 = \rho - \delta \tag{3.111}$$

And over again, we find an unstable chair approaching to our point Q_3.

3.6 STABILITY AND CHAOS

In this section, the values m, n and n_α for each critical point Q will be found, using the usual parameters for a laser with saturable filter; the system's behaviour will also be graphically presented

The values used[2] were as follows:

α	1.391
α_α	0.2
ρ	6.664
δ	9.89
G	160

Using the initial values found for Q_1 (3.41, 3.42 & 3.43) the behaviour observed is shown in figures 3.3, 3.4 and 3.5, with the following stability values

$$m_{q1} = 0.8121808153345$$

$$n_{q1} = 0.71267281106$$

$$n_{\alpha q1} = 0.18781918508$$

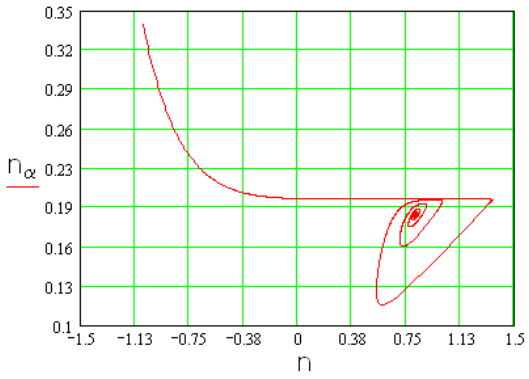

Figure 3.3 System's behaviour Graph (critical point Q_1) in the plane n,n_α

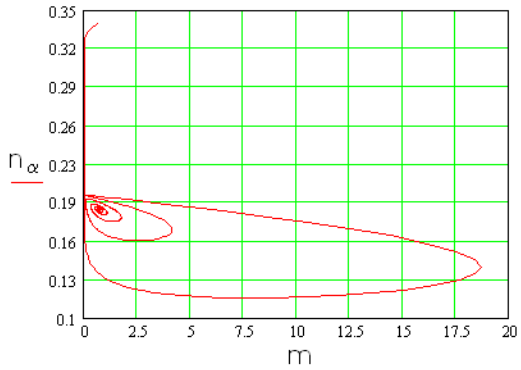

Figure 3.4 System's behaviour Graph (critical point Q_1) in the plane m,n_α

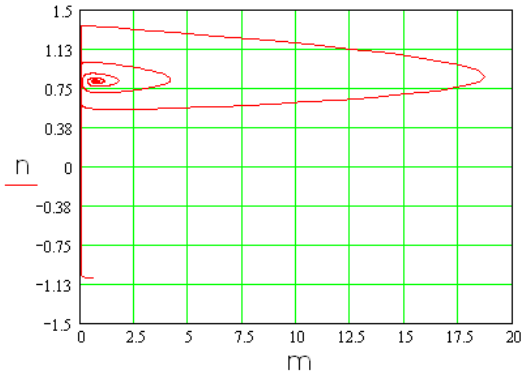

Figure 3.5 System's behaviour Graph (critical point Q_1) in the plane m,n

These graphs enable us to observe how the approximation towards the fixed point (m_{q1},n_{q1}, $n_{\alpha q1}$) resembles a simple attractor.

For the initial conditions given by equations (3.63), (3.64) & (3.65), the values obtained for the critical point Q_2 were:

$$m_{q2} = 0.62018363$$

$$n_{q2} = 0.858544673$$

$$n_{\alpha q2} = 0.1414562$$

The system's behaviour at point Q_2 is shown in figures 3.6, 3.7 y 3.8

Figure 3.6 System's behaviour Graph (critical point Q_2) in the plane n,n_α

Figure 3.7 System's behaviour Graph (critical point Q_2) in the plane m,n_α

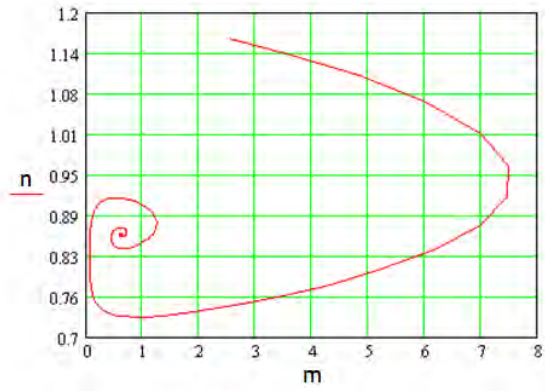

Figure 3.8 System's behaviour Graph (critical point Q_2) in the plane m,n

These graphs enable us to observe how the approximation towards the fixed point (m_{q2},n_{q2}, $n_{\alpha q2}$) resembles a stable spiral.

For critical point Q3, changing the initial conditions to (3.83), (3.84) & (3.85) we could not determine a fixed stability point as in figures 3.9, 3.10 and 3.11

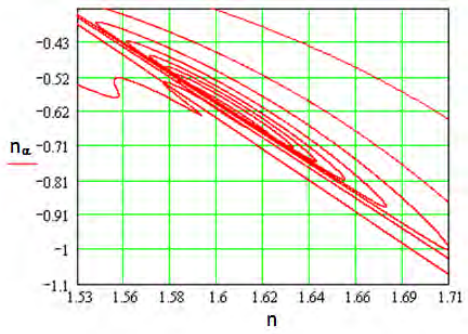

Figure 3.9 System's behaviour Graph (critical point Q_3) in the plane n,n_α

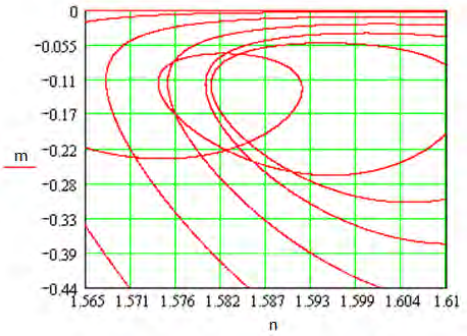

Figure 3.10 System's behaviour Graph (critical point Q_3) in the plane n,m

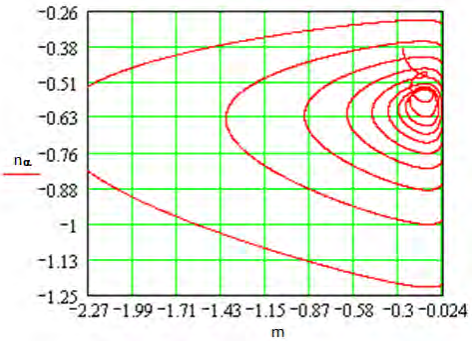

Figure 3.11 System's behaviour Graph (critical point Q_3) in the plane m,n_α

The graphs enable us to determine that the approximation to the point is as an instable node, as we approach the critical point a chaotic behaviour may be observed and will be studied in the next chapter.

3.7 THIRD CHAPTER REFERENCES

- [1] STATZ, H.; DE MARS, G. **"Transients and Oscillation Pulses in Masers"**. Quantum Electronics, 530-537, Columbia Univ. Press, New York, 1960
- V. ABOITES, **LASERES**, Ed. CIO, México, 1998
- [2] L. TARASSOV, **PHYSIQUE DES PROCESSUS DANS LES GÉNÉRATEURS DE RAYONNEMENT OPTIQUE COHÉRENT**, Ed. Mir, Moscow, 1981
- P. O'NEIL, **ADVANCED ENGINEERING MATHEMATHICS 5th**, Brooks Cole, USA, 2003
- G. B. ARFKEN, **MATHEMATICAL METHODS FOR PHYSICISTS 5th**, Harcourt Academic Press, USA, 2001
- D. W. JORDAN & P. SMITH, **NON LINEAR ORDINARY DIFFERENTIAL EQUATIONS**, Oxford university press, UK, 1979
- C. R. WYLIE, **DIFFERENTIAL EQUATIONS**, Mc. Graw-Hill, USA, 1979
- M. W. HIRSCH & S. SMALE, **DIFFERENTIAL EQUATIONS, DYNAMICAL SYSTEMS, AND LINEAR ALGEBRA**, Academic Press, inc., USA, 1974

CHAPTER 4

4.1 INTRODUCTION

In this chapter, we will explore a Statz-de Mars forced system. The chaos-state will be presented for two different settings. A future work outline will be considered and this thesis ends with a global conclusion of this work.

4.2 CHAOS RESULTS

In the previous chapter the Statz-de Mars equations for a laser with an intracavity saturable absorber was solved, the stability analysis was made, so that three stability points were found and the behavior of the solution in the neighborhood of those points was plotted; the non dimensional Statz-de Mars system is the following one:

$$\frac{dm}{dt'} = Gm(n + n_\alpha - 1)$$

$$\frac{dn}{dt'} = \alpha - n(m+1)$$

$$\frac{dn_\alpha}{dt'} = \alpha_\alpha \sigma - n_\alpha(\rho m + \delta)$$

The conditions needed to take the system to the chaotic behavior were given by the instability conditions, that is, when the system is not in one of its critical stable points; the instability was produced, moving away from the stable points, the used values are valid for a theoretical He-Ne laser and those values are the following ones:

α	4
α_α	61
ρ	0.001
δ	1
G	200

To be able to observe the chaotic behavior of the system under study, it was necessary to make a computer program in Mathcad professional 2001 (and in mathematica 5.0 for comparation); what this program does is to iterate the Statz-de Mars system, and give a plotting of

those points as an output. In the first try, 500 iterations were realized and 15,000 points were plotted in the results graphs, the initial conditions obtained from an instable state of the system used as seed to start the iterations were the following ones:

m	$\frac{\alpha + \alpha_\alpha - 1}{1 - \alpha_\alpha}$
n	$1 - \alpha_\alpha$
n_α	$\alpha_\alpha \left(1 - \frac{\rho}{\partial} \frac{\alpha + \alpha_\alpha - 1}{1 - \alpha_\alpha}\right)$

Under those conditions the time plots obtained for each variable were:

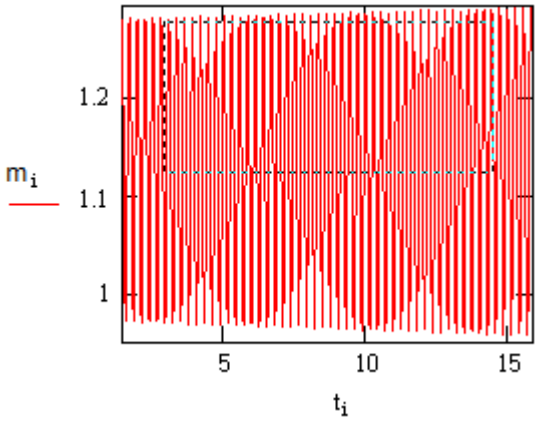

Figure 4.1 m against time after 500 iterations of the system. A periodic behavior can be observed, fulfilling the dense periodic property.

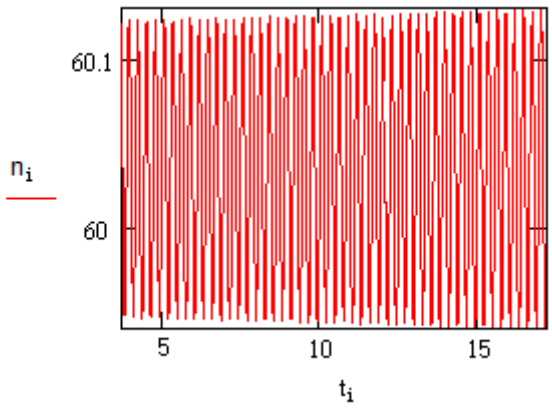

Figure 4.2 n against time after 500 iterations of the system. A denser periodic behavior is observed, fulfilling the same condition as in the above graph.

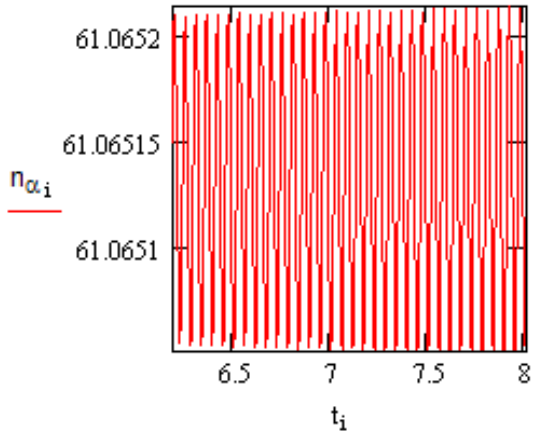

Figure 4.3 n_α against time after 500 iterations of the system. In the same way, a periodic behavior is observed.

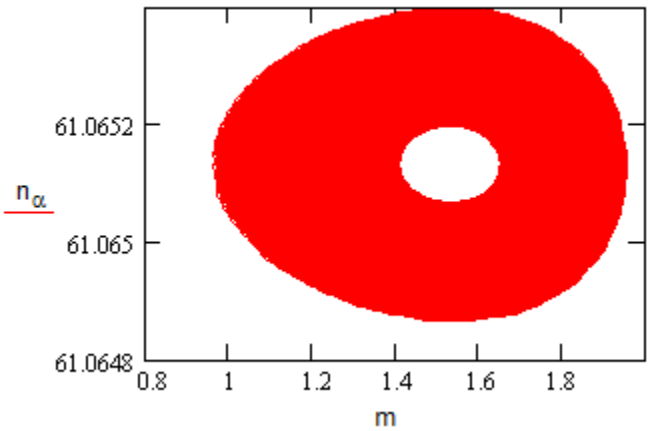

Figure 4.4 Full view of the plot for the (m, n_α) plane after 500 iterations of the system; Since this full view does not allow us to observe the behavior properly, a zoom to enable us a better examination, was made on a small region of the graph.

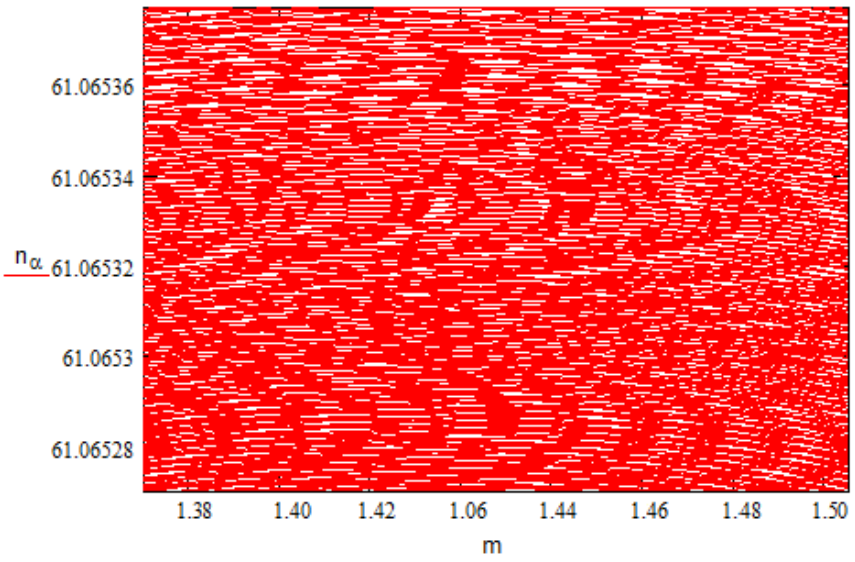

Figure 4.5 Zoom view for the plot of the (m, n_α) plane after 500 iterations of the system. the mixing of the intervals in this part of the graph can be fully appreciated.

For a better examination of the system behavior under the given conditions, an increase in the iterations number to 1500 was made, obtaining a better image of a strange attractor; the next zoomed image for the plane (m, n_α) proves it.

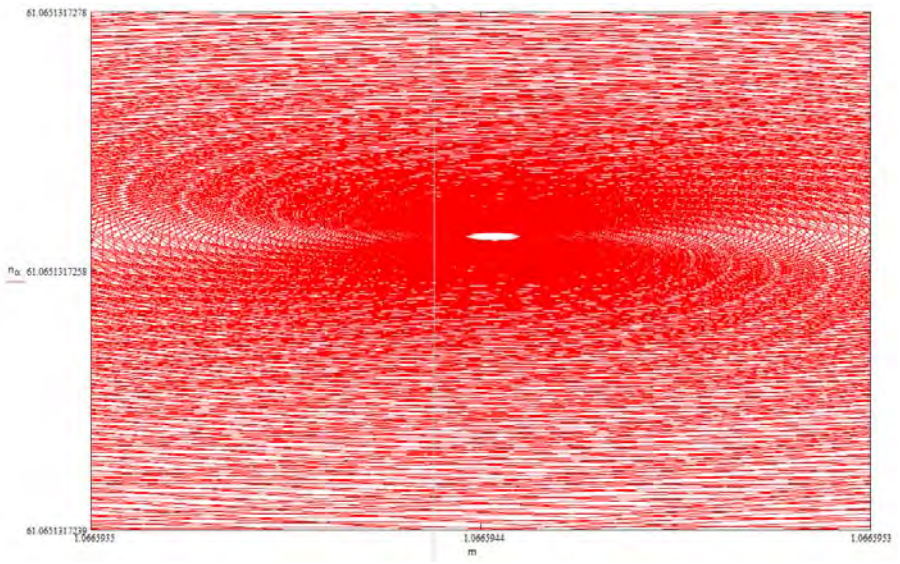

Figure 4.6 Mapping for the (m, n_α) plane, zoomed after 1500 iterations of the system. In this graph a dense periodic points and the mixing coexistence can be observed, showing that the system presents a deterministic chaotic behavior.

In order to complete the proof, advantage was taken of the hypersensibility to initial conditions that chaotic systems do present; summing one hundredth of a point to the initial conditions and, then, subtracting one hundredth of a point to the original values of the initial conditions used, the change was made, and the next time plots was obtained:

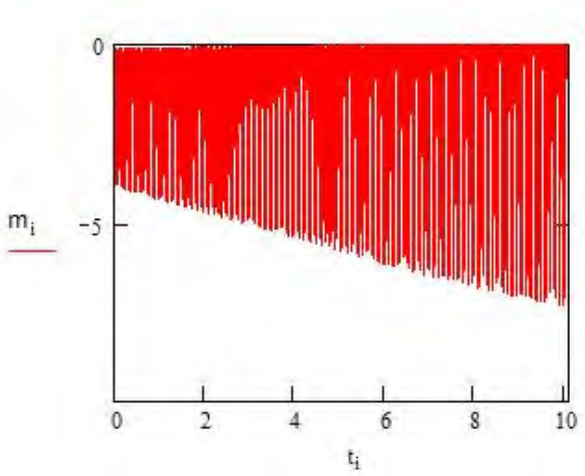

Figure 4.7 m against time after 500 iterations to the system when one hundredth is summed to the initial conditions of the system. In this graph, a noisy behavior, increasing through the time is observed

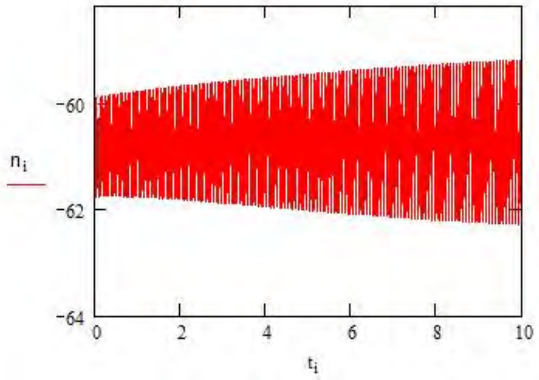

Figure 4.8 n against time after 500 iterations to the system when one hundredth is summed to the initial conditions of the system. A periodic behavior of the variable, increasing through the time can be observed.

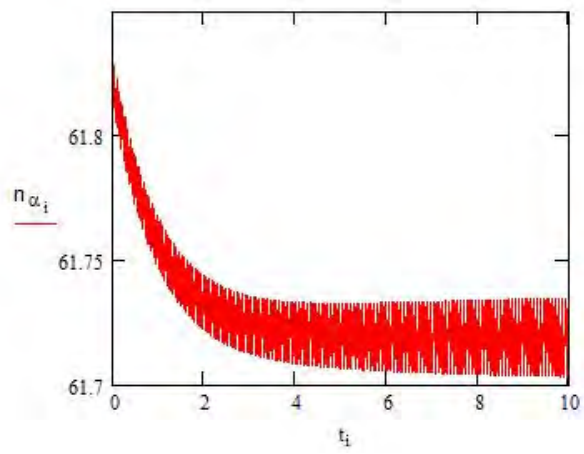

Figure 4.9 n_α against time after 500 iterations to the system with one hundredth summed to the initial conditions of the system. A periodic damped behavior of the variable can be observed a.

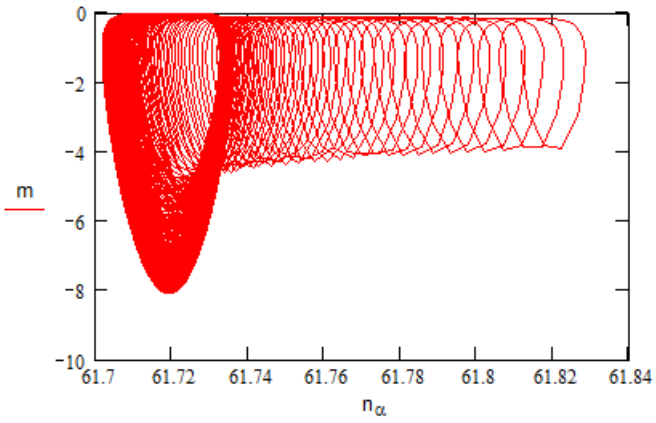

Figure 4.10 Plot with one hundredth summed to the initial conditions of the system for the (m, n_α) plane; full view. A chaotic image with a strange attractor was obtained.

In those graphs, a change on the behavior of the variables can be appreciated, as was to be expected; we now proceed to subtract one hundredth of a point from the initial conditions original values. The following graphs were obtained.

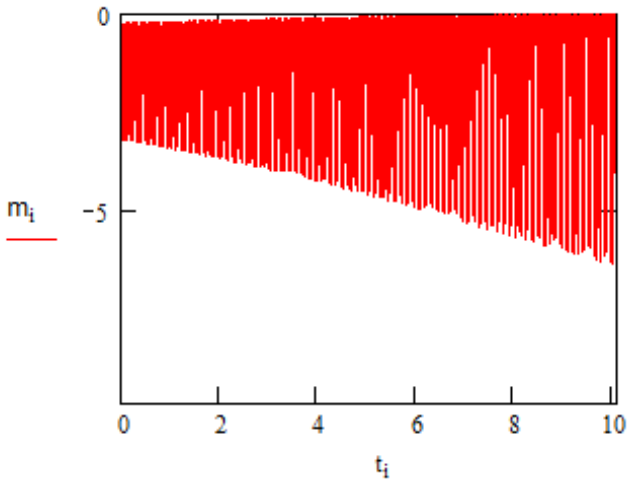

Figure 4.11 m against time after 500 iterations applied to the system with one hundredth subtracted to the initial conditions of the system. The behavior of the variable is similar only in the growing state to the same variable with the hundredth summed to the initial conditions.

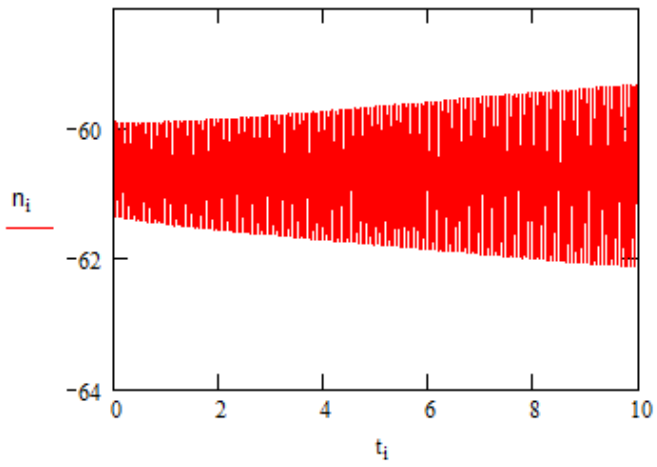

Figure 4.12 n against time after 500 iterations applied to the system with one hundredth subtracted to the initial conditions of the system. The behavior of the variable is similar only in the growing state to the same variable with the hundredth summed to the initial conditions, a denser behavior of the variable can be observed.

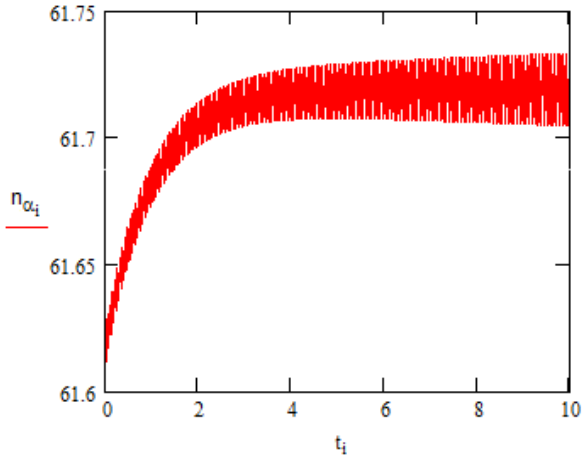

Figure 4.13 n_α against time after 500 iterations applied to the system with one hundredth subtracted to the initial conditions of the system. The behavior of the variable is inverted compared with the same variable with the hundredth summed to the initial conditions.

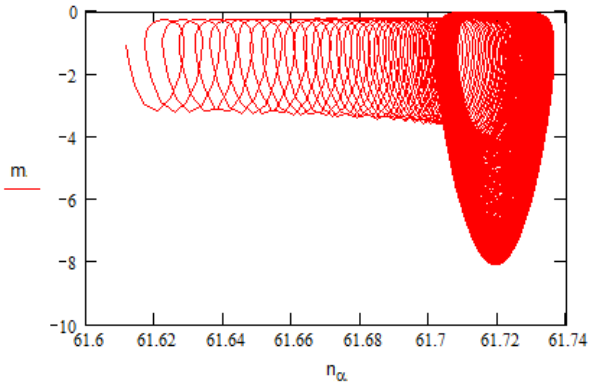

Figure 4.14 Plot with one hundredth subtracted to the initial conditions of the system for the (m, n_α) plane; full view. A chaotic image with a strange attractor was obtained; an inverted state, when comparing this graph with its homologue, clearly exists.

Trying to prove this strange behavior the 3-d plots were made for the two different configurations (with the hundredth summed and subtracted to the initial conditions) and they are as follows:

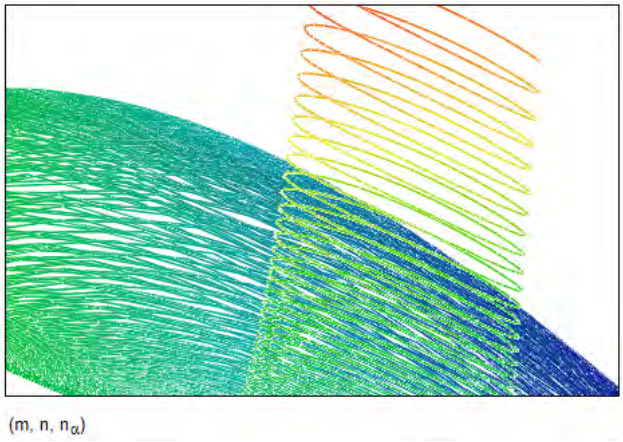

Figure 4.15 3d-plot with one hundredth point summed to the initial conditions of the system

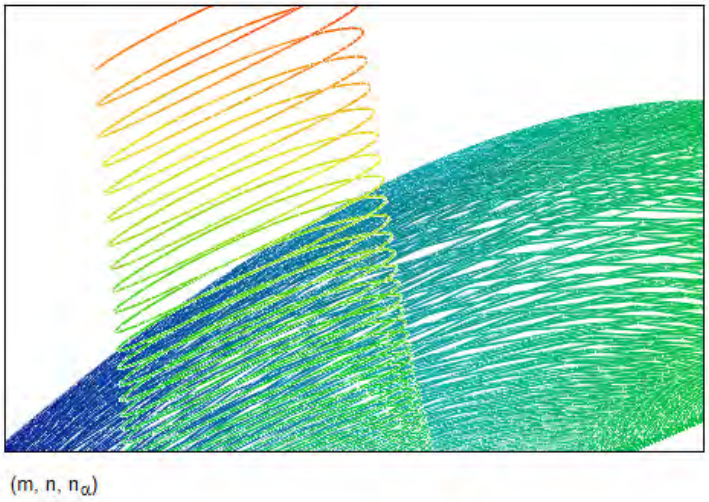

Figure 4.16 3d-plot with one hundredth point subtracted to the initial conditions of the system

From the graphics above we can conclude that the system is chaotic. A variation of ±0.01 was done obtaining, as expected, a different chaotical behavior; satisfying the sensitivity to initial conditions property. Also, the dense periodic points appeared in all the graphics, satisfying that property; and, the mixing property was present in all the plane plots; the unexpected fact was the "mirror chaos" due to the sign difference on the saturable absorber initial condition.

4.3 FINAL CONCLUSIONS

The realization of this work allows the following conclusions to be drawn:

- Even though a laser resonator with a saturable absorber normally after an interval of time has a tendency to stabilize, certain parameters can be found to produce chaos in the cavity.
- To find chaos in a three-level laser resonator it is imperative to force the Statz-de Mars equations using as the initial conditions for the equations system the values obtained for the bifurcation points (critical points), and as adimensional parameters the critical values that caused instability in the equations system.
- The region that presents chaos in the laser is always bounded.
- In the laser resonator we were able to find a “mirror chaotic” behavior, because the mirror happened to be one of the critical points.
- In the threshold of chaos the system possesses two single attractors and an unstable node corresponding to the critical points.

4.4 FUTURE WORK

This work opens a very wide window of possibilities for future research. The restlessness to verify in the laboratory the possibility to use “mirror chaos” as an algorithm to modulate and demodulate information sprung with it. It is the intention to find a practical use for the results presented here, using a laser resonator combined with a chaos generating element (e.g. a programmable saturable absorber). It also presents the possibility of taking advantage of the “high stability” zones founded in the chapter 3 of this thesis; in those zones, a quasi perfect spatial-temporal coherence can be achieved with a laser beam. These results still are to be corroborated in the laboratory.

The obtained results incite us to investigate with other laser elements (e.g. thin films and choppers) looking for points of special interest (e.g. stable, unstable, chaotic and bifurcation) with the zeal to contribute to a better laser knowledge and therefore to make a better use of the laser devices.

4.5 Fourth Chapter references

- L. TARASSOV, **PHYSIQUE DES PROCESSUS DANS LES GÉNÉRATEURS DE RAYONNEMENT OPTIQUE COHÉRENT**, Éditions MIR, 1981
- K. T. ALLIGOOD & CO., **CHAOS: AN INTRODUCTION TO DYNAMICAL SYSTEMS**, Springer, 1996
- J. CHANDRA, **CHAOS IN NONLINEAR DYNAMICAL SYSTEMS**, Siam, 1984
- C. S. DESAI & J. F. ABEL, **INTRODUCTION TO THE FINITE ELEMENT METHOD**, Van Nostrand Reinhold Company, 1972
- R. H. ENNS & G. C. MCGUIRE, **NON LINEAR PHYSICS WITH MATHEMATICA FOR SCIENTISTS AND ENGINEERS**, Birkhäuser, 2001
- D. DUBIN, **NUMERICAL AND ANALYTICAL METHODS FOR SCIENTIST AND ENGINEERS USING MATHEMATICA**, Wiley, 2003